Different acyl-CoA:diacylglycerol acyltransferases vary widely in function, and a targeted amino acid substitution enhances oil accumulation

Hatanaka, Tomoko ; Tomita, Yoshiki ; Matsuoka, Daisuke ; Sasayama, Daisuke ; Fukayama, Hiroshi ; Azuma, Tetsushi ; Soltani Gishini,…

(Citation)
Journal of Experimental Botany,73(9):3030-3043

(Issue Date)
2022-03-04

(Resource Type)
journal article

(Version)
Accepted Manuscript

Photos of oil crops; Vernonia (*Vernonia galamensis*), sunflower (*Helianthus annuus*), Jatropha (*Jatropha curcas*), and castor bean (*Ricinus communis*). Acyl-CoA:diacylglycerol acyltransferase type 1 (DGAT1) plays a pivotal role to accumulate triacylglycerol (TAG) as a storage lipid. The yeast expression experiment results imply that DGAT1s from Vernonia, sunflower, Jatropha, and sesame are highly active, while DGAT1s from Arabidopsis, soybean, and castor bean are much less active than former four species.

Title

Different acyl-CoA:diacylglycerol acyltransferases vary widely in function and a targeted amino acid substitution enhances oil accumulation

Authors

Tomoko Hatanaka[1,‡], Yoshiki Tomita[1], Daisuke Matsuoka[1,*], Daisuke Sasayama[1], Hiroshi Fukayama[1], Tetsushi Azuma[1], Mohammad Fazel Soltani Gishini[2], David Hildebrand[3]

1 Graduate School of Agricultural Science, Kobe University, Kobe, Hyogo, Japan, 675-8501
2 Department of Production Engineering and Plant Genetics, Faculty of Sciences and Agricultural Engineering, Campus of Agriculture and Natural Resources, Razi University, Kermanshah, Iran
3 Department of Plant and Soil Sciences, University of Kentucky, Lexington, KY, USA, 40546-0312

*Present address: Division of Food Design, Faculty of Nutrition, Koshien University, Takarazuka, Hyogo, Japan, 665-0006, matsuoka@koshien.ac.jp

‡Correspondence: thata@kobe-u.ac.jp

Running title

A targeted amino acid substitution improves DGAT1 potentials

Highlight

Seven *DGAT1s* were tested for their effects on TAG accumulation in Arabidopsis and yeast. They were divided into high and low function and a site-directed mutagenesis enhanced function in yeast.

Abstract

Triacylglycerols (TAGs) are the major component of plant storage lipids such as oils. Acyl-CoA:diacylglycerol acyltransferase (DGAT) catalyzes the final step of the Kennedy pathway, and is mainly responsible for plant oil accumulation. We previously found that the DGAT activity of Vernonia DGAT1 was distinctively higher than that of Arabidopsis and soybean DGAT1 in a yeast microsome assay. In this study, the *DGAT1* cDNAs of Arabidopsis, Vernonia, soybean, and castor bean were introduced into Arabidopsis. All Vernonia *DGAT1*-expressing lines showed a significantly higher oil content (49% mean increase compared with the wild-type) followed by soybean and castor bean. Most Arabidopsis *DGAT1*-overexpressing lines did not show a significant increase. In addition to these four *DGAT1*s, sunflower, Jatropha, and sesame *DGAT1* genes were introduced into a TAG biosynthesis-defective yeast mutant. In the yeast expression culture, DGAT1s from Arabidopsis, castor bean, and soybean only slightly increased the TAG content; however, DGAT1s from Vernonia, sunflower, Jatropha, and sesame increased TAG content >10-fold more than the former three DGAT1s. Three amino acid residues were characteristically common in the latter four DGAT1s. Using soybean *DGAT1*, these amino acid substitutions were created by site-directed mutagenesis and substantially increased the TAG content.

Keywords: Acyl-CoA:diacylglycerol acyltransferase, *Arabidopsis thaliana*, DGAT1, site-directed mutagenesis, triacylglycerol, *Vernonia galamensis*, yeast strain H1246

Introduction

Vegetable oil is one of the most important renewable resources in the world. In addition to a wide range of food applications, vegetable oils are also valuable as renewable chemical derivatives such as lubricants, paints, adhesives, varnishes, plasticisers, and biodiesel (Carlsson, 2009; 2011; Jaworski and Cahoon, 2003; Ohlrogge, 1994). Triacylglycerol (TAG) is a major component of plant storage lipids and is synthesized by continuous esterification of acyl chains from acyl-CoA at the *sn*-1, -2, and -3 positions of the glycerol backbone (Ohlrogge and Browse, 1995).

Three types of enzymes were identified that catalyze the final stage of TAG synthesis: acyl-CoA: diacylglycerol acyltransferase (DGAT) (Cases *et al.*, 1998; Hobbs *et al.*, 1999; Zou *et al.*, 1999), phospholipid: diacylglycerol acyltransferase (PDAT) (Dahlqvist *et al.*, 2000; Oelkers *et al.*, 2000; Stahl *et al.*, 2004) and diacylglycerol transacylase (DAG transacylase) (Fraser *et al.*, 2000; Stobart *et al.*, 1997). Of these enzymes, DGAT is the most important and has been suggested to be the rate-determining factor in TAG synthesis. In eukaryotes, several classes of DGATs have been identified based on differences in structure and activity (He *et al.*, 2004; Lung and Weselake, 2006). DGAT1 belongs to the membrane-bound *O*-acyltransferase (MBOAT) family (Cases *et al.*, 1998), and is usually predicted to have nine or 10 transmembrane domains in higher plants. The gene encoding *DGAT1* has been isolated and characterized from many plant species (Banilas *et al.*, 2011; Beisson *et al.*, 2003; Bouvier-Nave *et al.*, 2000; Hatanaka *et al.*, 2003; Hobbs *et al.*, 1999; Jako *et al.*, 2001; Li *et al.*, 2013b; Li *et al.*, 2010a; Nykiforuk *et al.*, 2002; Shockey *et al.*, 2006; Tuechetto-Zolet *et al.*, 2011; 2008; Yu *et al.*, 2006). The DGAT2 protein has two predicted transmembrane domains and belongs to the monoacylglycerol acyltransferase (MGAT) family. Both DGAT1 and DGAT2 are endoplasmic reticulum (ER) membrane-binding enzymes; however, their amino acid sequences are not homologous to each other (Bates, 2016; Cases *et al.*, 2001; He *et al.*, 2004; Kroon *et al.*, 2006; Lardizabal *et al.*, 2001; Shockey *et al.*, 2006; Xu *et al.*, 2013). DGAT2 from some species is reported to contribute to the accumulation of unusual fatty acids such as a hydroxy fatty acid (ricinoleic acid) in castor bean (*Ricinus communis*) (Burgal *et al.*, 2008; Cagliari *et al.*, 2010; Kroon *et al.*, 2006; Regmi *et al.*, 2020; Shockey *et al.*, 2019; Troncoso-Ponce *et al.*, 2011), a conjugated fatty acid (α-eleostearic acid) in tung tree (*Vernicia fordii)* (Shockey *et al.*, 2006), and an epoxy fatty acid (vernolic acid) in Vernonia (*Vernonia galamensis*) (Li *et al.*, 2010b). DGAT1 and DGAT2 are ER membrane-bound, whereas DGAT3 is a soluble cytoplasmic enzyme identified in peanuts (*Arachis hypogaea*) (Saha *et al.*, 2006), *Arabidopsis thaliana* (Hernandez *et al.*, 2012), and upland cotton (*Gossypium hirsutum*) (Zhao *et al.*, 2021). A fourth type of DGAT has a sequence similar to DGAT2 and has both wax ester synthase (WS) and DGAT activity (WS / DGAT) (Kalscheuer and Steinbuchel, 2003; King *et al.*, 2007; Li *et al.*, 2008; Rosli *et al.*, 2018; Xu *et al.*, 2021). The most common DGAT is type 1 (DGAT1), which contributes to most of the TAG synthesis in higher plants (Chen *et al.*, 2016; Sanjaya *et al.*, 2013; Xu *et al.*, 2018a), but DGAT2 plays a major role in castor bean (Burgal *et al.*, 2008; Kroon *et al.*, 2006; Troncoso-Ponce *et al.*, 2011) and tung tree (Shockey *et*

al., 2006), and DGAT3 is expressed highly in upland cotton (Zhao *et al.*, 2021). Many studies have reported that increased expression of the *DGAT1* gene increases oil content (Andrianov *et al.*, 2010; Lardizabal *et al.*, 2008; Rao and Hildebrand, 2009; Taylor *et al.*, 2009).

Vernonia galamensis is an annual herbaceous plant native to East Africa belonging to the Asteraceae family. It contains ~40% oil in its seeds and is known to be an epoxy fatty acid accumulator (Ayorinde *et al.*, 1988; Carlson and Chang, 1985; Perdue *et al.*, 1986). Vernonia seed oil contains up to 80% vernolic acid (*cis*-12,13-epoxy-*cis*-9-octadecenoic acid) (Anderson *et al.*, 1993; Neff *et al.*, 1993). From Vernonia developing seeds, two types of *DGAT1* genes (*VgDGAT1A* and *VgDGAT1B*) have been isolated and their various characteristics have been investigated (Hatanaka *et al.*, 2003; Yu *et al.*, 2008). Expression of the *Stokesia laevis* epoxygenase gene in soybean seeds showed undesirable phenotypic changes in the transformed seeds such as wrinkles and weight reduction. However, these negative side effects were restored by co-expression with *VgDGAT1A* (Li *et al.*, 2012). Even though Vernonia DGAT2 is more effective than DGAT1s in vernolic acid accumulation (Li *et al.*, 2010b), VgDGAT1A also significantly increased vernolic acid accumulation in soybean seeds.

In our previous study, in a microsome assay using an expression system in wild-type yeast (*Saccharomyces cerevisiae*), Vernonia DGAT1 was ~40 times more active than Arabidopsis DGAT1 and about nine times more active than soybean (*Glycine max*) DGAT1 (Hatanaka *et al.*, 2016). However, in this system using wild-type yeast (INVSc1, Invitrogen), the activity of *A. thaliana DGAT1* was close to that of the vector control. Therefore, it is unclear whether the activity of DGAT1 expressed in wild-type yeast would match these results when it is expressed in plants.

In this study, the effectiveness of DGAT1s among plant species was investigated. The *DGAT1* genes evaluated were derived from four species: *V. galamensis*, soybean (*G. max*), castor bean (*R. communis*), and *A. thaliana*. The genes were overexpressed in Arabidopsis, and their effects on the seed oil content and fatty acid composition were investigated. A further three *DGAT1* cDNAs were obtained from sunflower (*Helianthus annuus*), Jatropha (*Jatropha curcas*), and sesame (*Sesamum indicum*), and these seven DGAT1 genes were expressed in the yeast quadruple mutant H1246 strain (*S. cerevisiae*) (Sandager *et al.*, 2002), which is deficient in TAG synthesis, and their TAG contents were measured. The amino acid sequence of sunflower DGAT1 is very close to that of Vernonia DGAT1s, and there are reports that Jatropha *DGAT1* (Misra *et al.*, 2013) and sesame *DGAT1* (Wang *et al.*, 2014) are effective for increasing the seed oil contents of transgenic *A. thaliana* lines expressing these genes. In addition, direct protein engineering has been used to generate DGAT1 variants with enhanced activity (Roesler *et al.*, 2016; Siloto *et al.*, 2009). Chen *et al.* (2017) reported that a single amino acid residue substitution leads to enhanced *Brassica napus* DGAT1 activity in yeast. Herein, we aim to clarify the diversity of DGAT1 properties among plant species, and find factor(s) to increase their effectiveness of DGAT1s in TAG accumulation.

Materials and methods

DGAT1 cDNA cloning and the construction of plant and yeast expression vectors

Total RNAs were extracted from developing seeds of *A. thaliana* (ecotype, Col-0), soybean (cv. Jack), castor bean, Jatropha, and sesame (cv. Kanto-1) using an RNeasy Plant Mini Kit™ according to the manufacturer's instructions (Qiagen, https://www.qiagen.com). Reverse transcription of RNAs was carried out using a PrimeScript II first strand cDNA Kit™ (Takara Bio, Japan). The coding sequences of *DGAT1s* were amplified by a high-fidelity KOD-Plus-Neo polymerase (Toyobo, Japan) using end-specific primers containing restriction sites. The GenBank numbers of DGAT1 genes in this study are listed in Supplementary Table S1. The primers used in this section are listed in Supplementary Table S2-1. Seeds of sesame (cv. Kanto-1) were gifted from the National Agriculture and Food Research Organization (NARO) Genebank, Japan. Seeds of Jatropha were gifted from Dr. Kazuo Sambongi, Director of NIPPON BIODIESEL FUEL Co., Ltd.

.

Arabidopsis transformation and growth conditions

For plant expression the amplification products, *AtDGAT1*, *GmDGAT1A*, and *RcDGAT1* were subcloned into the respective sites of the pPHI4752 vector containing a phaseolin promoter, which confers strong seed-specific expression of transgenes (Bustos *et al.*, 1998; Kawagoe *et al.*, 1994). The phaseolin promoter cassette containing the coding region of each target gene was transferred into the corresponding sites of the binary pCAMBIA1301, T-DNA vector (Cosmo Bio, Japan). Regarding *VgDGAT1A*, the vector constructed in the previous study (Li *et al.*, 2012) was used.

The recombinant plasmids were transformed into *Agrobacterium tumefaciens* strain EHA105 by the freeze-thaw method. Transformation of *A. thaliana* (ecotype Col-0) plants was carried out using the floral dip method (Clough and Bent, 1998). T_1 seeds were grown on a solid selection medium composed of MS salts (Murashige and Skoog, 1962), B5 vitamins (Gamborg *et al.*, 1968), 1% (w/v) sucrose, 25 mg l^{-1} (w/v) hygromycin, and 0.8% agar. Plants were grown in a culture room at 23°C under long-day conditions (16 h of light/8 h of dark) at a photon flux density of 90 μmol m^{-2} s^{-1}. T_2 seeds were harvested and the seeds were checked for total lipid and TAG contents. Two individual transgenic lines into which each *DGAT1* gene was introduced were selected and grown under the same conditions described above. The developing siliques of T_2 generations were used for quantitative PCR (qPCR) and the mature T_3 seeds were used for lipid analysis.

Yeast transformation and culture

For the yeast expression system, coding regions of *DGAT1*s (*AtDGAT1*, *RcDGAT1*, *GmDGAT1A*, *VgDGAT1A*, *HanDGAT1*, *JcDGAT1*, and *SiDGAT1*) were cloned into the yeast vector pYES2 (Invitrogen). *S. cerevisiae* strains were then transformed with the experimental constructs using the lithium acetate-mediated method as well as an empty vector control. The *S. cerevisiae* strains used in

this study were the quadruple knock-out strain H1246 (*MATa are1-D::HIS3, are2-D:: LEU2, dga1-D::KanMX4*, and *lro1-D::TRP1 ADE2*), containing knockouts of all four neutral lipid biosynthesis genes *DGA1, LRO1, ARE1*, and *ARE2*, kindly distributed by Dr. S. Stymne (Sandager *et al.*, 2002). All transformants were selected on synthetic complete medium lacking uracil (SC-U, 6.7% (w/v) of Yeast Nitrogen Base, 0.01% (w/v) of adenine, arginine, cysteine, leucine, lysine, threonine and tryptophane; 0.050% (w/v) of aspartic acid, histidine, isoleucine, methionine, phenylalanine, proline, serine, tyrosine, and valine) supplemented with 2% (w/v) glucose and 2% (w/v) agar. The recombinant yeast cells were cultivated in a liquid medium according to the manufacturer's instructions. The induction culture was performed at 30°C with shaking at 180 rpm in the dark for 5 d to reach the stationary phase. The expression of transgenes was checked by reverse transcription-PCR (RT-PCR). Total RNA extraction and the first strand cDNA synthesis were carried out by the same method described above. Primer sequences for *DGAT1* inside fragments and yeast *Actin1* as an internal reference gene are shown in Supplementary Table S2-2.

Quantitative RT-PCR

The relative transcript levels of DGAT1 genes were analyzed by RT-qPCR. RNAs were isolated from 50−100 mg of Arabidopsis immature siliques or 2 d induced cultured yeast using an ISOSPIN Plant RNA Kit™ (Nippon Gene, Japan). The reverse transcription reaction was carried out using a PrimeScript II first strand cDNA Kit™ (Takara Bio, Japan) for Arabidopsis or a PrimeScript IV first-strand cDNA synthesis Kit™ (Takara Bio, Japan) for yeast. RT-qPCR (qPCR) was performed using a MyGo Pro Real Time PCR System (Funakoshi, Japan).

For Arabidopsis, the 12.5 µl reaction mixtures contained 0.4 µM of each specific oligonucleotide primer for the *DGAT1* or Arabidopsis *Actin2* (*AtACT2*) as the reference gene, 6.25 µl of SYBR Green Premix EX Taq GC™ (Takara Bio, Japan) and ~100 ng cDNA according to the manufacturer's instructions. Thermal parameters for amplification were 95°C for 10 min followed by 45 cycles of 95°C for 30 s and 60°C for 60 s. Because endogenous Arabidopsis *DGAT1 (AtDGAT1)* of immature siliques showed a stable expression level which was calculated relative to *AtACT2* in the wild-type and all transgenic plants, we thought the expression levels of exogenous *DGAT1*s should be reliable. These results are listed in the Supplementary Table S3.

For the yeast qPCR assays, the 20 µl reaction mixtures contained 0.4 µM of each specific oligonucleotide primer for *DGAT1* or yeast *Actin1* (*ScACT1*) and yeast *18S rRNA* (*ScRDN18*) as the reference genes and 10 µL KOD SYBR qPCR Mix (Toyobo, Japan) according to the manufacturer's instructions. When *ScRDN18* was used as a reference gene, the template cDNA was diluted to 1/1000. Thermal parameters for amplification were 98°C for 2 min followed by 45 cycles of 98°C for 10 s, 60°C for 10 s and 68°C for 30 s. Melting curves were performed immediately after the completion of the RT-qPCR, and the fluorescence was measured from 60°C to 97°C. Transcript abundances were normalized with respect to the reference genes. The expression levels of transcripts were calculated relative to the reference gene according to the equation: relative expression = $2^{-\Delta Cq}$,

where ΔCq = Cq(target) – Cq(reference). The mean values of three technical replicates was used for each biological replicate. The oligonucleotide primer sequences are shown in Supplementary Table S2-2.

Site-directed mutagenesis of GmDGAT1A

Single amino acid residue substitutions and site-saturation mutagenesis at sites 149, 205, or 263 were introduced into the native GmDGAT1A. Briefly, the full length of the native *GmDGAT1A* coding region was cloned into a pGEM^{R}-T Easy Vector (Promega, USA). Site-directed mutagenesis was performed by inverse PCR using PrimeSTAR GXL polymerase (Takara, Japan) and the pGEM^{R}-T-vector as a template. The mutagenic primers were designed to change phenylalanine to leucine (F149L), phenylalanine to valine (F205V), or alanine to valine (A263V). These primer sequences are shown in Supplementary Table S2-2. The full length of the coding region in the pGEM^{R}-T-vector was sequenced and single site mutagenesis was confirmed. To construct double- and triple-site mutants, a single site-mutated *GmDGAT1A* and a double site-mutated *GmDGAT1A* were used as a template, respectively. The single site-mutated *GmDGAT1A* variants were introduced into yeast H1246 and cultured as described above. The *HanDGAT1* introduced line was also cultured as an example of highly active DGAT1.

Lipid analysis

Lyophilised Arabidopsis mature seeds or yeast cells induction-cultured for 5 d were lyophilised and triheptadecanoin (tri-17:0) was added at 10 μg mg^{-1} tissue as a standard. The samples were finely ground with a mortar and pestle with 2–3 mL of chloroform and methanol (2:1, v/v) containing 0.001% butylated hydroxytoluene (BHT). After a brief centrifugation, the chloroform phase was transferred into a new glass tube. Samples were divided into two aliquots. One was used for thin layer chromatography (TLC) and the other directly for gas chromatography (GC) analysis.

TLC was applied to separate individual lipid classes. The chloroform extracts were loaded on lanes of LK6D Silica gel 60A TLC plates (GE Healthcare Japan Co. Ltd, Tokyo, Japan), and the plates were put in a chamber with hexane:diethyl ether:acetic acid (80:20:1, v/v/v) containing 0.001% BHT. After chromatography, the plates were dried and then sprayed with 0.005% primulin in 80% acetone, followed by visualization under UV light. The TAG bands were scraped and transferred to a glass tube. The TAGs were eluted three times with 2 ml of diethyl ether.

For GC analysis, the samples were completely dried under an N_2 stream and mixed with 0.5 ml of 18 mg ml^{-1} sodium methoxide ($NaOCH_3$) in methanol and then incubated for 45 min with shaking at room temperature. Each dried sample was resolved in 2 ml of hexane containing 0.001% BHT. Then, the hexane layer was extracted and concentrated under an N_2 stream. Finally, the fatty acid methyl esters were analyzed with GC on a GC-14B (Shimazu Co. Ltd., Kyoto, Japan) with a 2.1 m×0.25 mm glass column filled with Unisole 3000 (GL Sciences Co Ltd., Tokyo, Japan) and a flame ionization detector (GC-FID).

Bioinformatics

The three-dimensional structures of VgDGAT1A, GmDGAT1A and GmDGAT1A-F146L were analyzed by I-TASSER (Yang and Zhang, 2015) and COFACTOR (Zhang *et al.*, 2017) based on a comparison with human DGAT1 (Wang *et al.*, 2020).

Results and discussion

Extent of transgenic Arabidopsis seed oil increase was dependent on the specific DGAT1 introduced

To test the results of our previous yeast microsome assay using AtDGAT1, GmDGAT1A, and VgDGAT1A *in planta*, cDNAs of *AtDGAT1*, *GmDGAT1A,* castor bean *DGAT1* (*RcDGAT1*), and *VgDGAT1A* were introduced into *A. thaliana* (Col-0) under the control of a seed-specific promoter. We obtained 11 to 16 transgenic lines from each of the introduced *DGAT1*s, and each T2 seed oil contents were measured (Supplementary Fig. S1). All T_2 seeds with *VgDGAT1A* showed higher oil contents than the wild-type seeds. Two transgenic lines from each *DGAT1* introduced were selected, and those T3 lines were designated as AtD-OE-4, AtD-OE-6 (*AtDGAT1* overexpression), GmD-1, GmD-3 (*GmDGAT1A*), RcD-4, RcD-10 (*RcDGAT1*), and VgD-10, VgD-12 (*VgDGAT1A*). Oil content and fatty acid composition of T_3 seeds from transgenic lines were analyzed by GC. T_3 seeds of VgD-10 and VgD-12 showed the highest seed oil contents (44% mean increase compared to the wild-type) followed by GmD-1, GmD-3 (32% increase), RcD-10, and RcD-4 (22% increase). VgD lines always showed significantly higher seed oil accumulation than wild-type plants (Fig. 1A). AtD-OE lines showed a small increase (Fig. 1A) even though the mRNA expression levels were 30-fold higher than the wild-type (Supplementary Table S3). These results reflected our previous yeast microsome assay study (Hatanaka *et al.*, 2016). The fatty acid compositions did not change drastically between wild-type plants and transgenic lines (Fig. 1B).

In yeast H1246, DGAT1s from seven species were roughly classified into two groups

Because the yeast expression system predicted the function of DGAT1s in plants, we tested more *DGAT1*s from other plant species to investigate how the DAGT1 functions differed among the species. We used yeast because the results could be obtained sooner than in plants. In addition to the four *DGAT1*s above, sunflower DGAT1 (*HanDGAT1*), Jatropha DGAT1 (*JcDGAT1*), and sesame DGAT1 (*SiDGAT1*) were introduced into the yeast quadruple knockout strain H1246. Transgenic yeast lines were designated 'VC' for an empty vector control, 'At' for *AtDGAT1*, 'Rc' for *RcDGAT1*, 'Gm' for *GmDGAT1A*, 'Vg' for *VgDGAT1A*, 'Ha' for *HanDGAT1*, 'Jc' for *JcDGAT1*, and 'Si' for

SiDGAT1. Because there are no codon usage biases between higher plants and *S. cerevisiae* (Appendix S1), the original plant *DGAT1* genes were introduced.

After 2 d, cultured cells were harvested for RT-PCR and RT-qPCR to check the gene expression. All introduced gene expressions were confirmed by RT-PCR (Supplementary Fig. S2).

After 5 d, cultured cells were harvested and submitted for lipid analysis. The TLC results showed that species could be classified into a low TAG accumulating group (At, Rc, and Gm) and a high TAG accumulating group (Vg, Ha, Jc, and Si) (Supplementary Fig, S3). We designated them the 'Low' group for the former three and the 'High' group for the latter four. Their total lipid and TAG contents were measured by GC (Fig. 2A). These results were supported by the image of the TLC analyses (Supplementary Fig. S3). The results from qPCR showed no correlation between the gene expression levels and the TAG accumulation levels (Supplementary Fig. S4). Fatty acid compositions were also significantly different between the two groups. For example, the level of palmitic acid (16:0) was higher and that of palmitoleic acid ($16:1^{\Delta 9}$) was lower in the 'High' group than the 'Low' group (Fig. 2B). In yeast culture cells that accumulated a significant amount of TAG, the TAG constituted a high proportion of the total lipids. Differences in the levels of stearic acid (18:0) were a little higher in the 'High' group than in the 'Low' group. These differences suggested that the increased TAG in the 'High' group had a different fatty acid composition compared to the total fatty acids of VC, which is expected to consist mainly of polar lipids. Because no fatty acid or lipid was supplemented in the induction cultures, the introduction of the 'High' group's *DGAT1* might have altered the distribution of fatty acids in yeast cells.

As we mentioned in the Introduction, our previous microsome assay using an expression system in wild-type yeast (INVSc1, Invitrogen) showed that GmDGAT1A exhibiting twice the activity of the controls and VgDGAT1A showed a 6-fold activity over GmDGAT1A, but AtDGAT1 did not show a significant difference compared with the vector control (Hatanaka *et al.*, 2016). In the current study, the quadruple knockout strain H1246 was used because the accumulated TAGs can be clearly observed (Sandager *et al.*, 2002). In addition, the results showed the yeast contained only four kinds of fatty acids (16:0, $16:1^{\Delta 9}$, 18:0, and $18:1^{\Delta 9}$). However, Brassicaceae plants may prefer to use very-long-chain fatty acids, such as $20:1^{\Delta 11}$ or $22:1^{\Delta 13}$ (Furmanek *et al.*, 2014; McGinn *et al.*, 2019; Xu *et al.*, 2008). The wild-type soybean seeds accumulate $18:2^{\Delta 9,12}$ as major fatty acid (Hatanaka *et al.*, 2016; Li *et al.*, 2013a; Li *et al.*, 2012). The acyl-CoA and DAG pools in yeasts may be one of the reasons that AtDGAT1 and GmDGAT1A are in the 'Low' group.

Three amino acid residues in the conserved region differed between the 'High' and 'Low' groups

In order to find the difference in protein levels between the 'High' and 'Low' group, we thoroughly studied their amino acid sequences. Figure 3 shows the amino acid sequence alignment of the conserved region of the DGAT1s tested in the yeast expression culture and rapeseed (*B. napus*) BnaDGAT1. The sequence of BnaDGAT1 is close to AtDGAT1 because they both belong to the

Brassicaceae family. BnaDGAT1 is well studied (Chen *et al.*, 2017), so it was added as a reference. The upper four DGAT1s shown in red letters were in the 'High' group. A comparison between the upper four and the lower four DGAT1s showed that three amino acid sites were different at (1), (2), and (3) in Fig. 3. In VgDGAT1A of the 'High' group, leucine (L) was at site 174, valine (V) at 230, and valine (V) at 288, whereas phenylalanine (F) was at site 149, phenylalanine (F) at 205, and alanine (A) 263 in GmDGAT1A of the 'Low' group. Corresponding sites of the other proteins are listed in Supplementary Table S4. Jatropha and castor bean both belong to the Euphorbiaceae family, and their full-length sequences are close (78.82% identity), but the three amino acid residues (1), (2), and (3) are different. Thus, these amino acids may cause the differences seen in TAG accumulation with the different DGAT1s. These three amino acids have not been referred to in previous reports of improving DGAT1s by amino acid substitution in GmDGAT1B (Roesler *et al.*, 2016) and BnaDGAT1 (Chen *et al.*, 2017).

In other oil crop DGAT1s, tung tree (*V. fordii*) DGAT1 (VfDGAT1) has the same three amino acid residues as the 'High' group, oil palm (*Elaeis guineensis*) DGAT1 (EgDGAT1) has leucine (L) at site 171, isoleucine (I) at site 227, and valine (V) at site 277; olive (*Olea europaea*) DGAT1 (OeDGAT1) has leucine (L) at site 183, valine (V) at site 238, and alanine (A) at site 297; and linseed (*Linum usitatissimum*) DGAT1 (OeDGAT1) has phenylalanine (F) at site 157, phenylalanine (F) at site 213, and valine (V) at site 271 (Supplementary Table S4). DGAT1s of olive and linseed may show medial characteristics between the 'High' group and the 'Low' group.

Black and blue lines in Fig. 3 indicate predicted trans-membrane helices (TMs) by Phobius. Most DGAT1s have nine TM helices (black lines), however DGAT1s of the Brassicaceae family have 10 TM helices (blue lines). The amino acid residue (1) is in the second TM helix (TM2), the residue (2) is in the fourth TM helix (TM4), and the residue (3) is in the cytosolic long loop (CL1) between TM4 and TM5 (Fig. 4A), however, a region around the residue (3) is within the fifth TM helix in Brassicaceae DGAT1s (Fig. 3).

A single amino acid substitution in GmDGAT1A increased TAG production

To analyze further the effect of amino acid residue substitutions of the DGAT1s of the 'Low' group on storage lipid biosynthesis, site saturation mutagenesis was performed at sites F149L, F205V, A263V, and their combinations in GmDGAT1A (Fig. 4B). All GmDGAT1A variants introduced into yeast H1246 lines accumulated higher TAG contents than the native GmDGAT1A line. In particular, F149L and A263V had a 4.95-fold higher TAG in F149L, and 3.99-fold higher TAG in A263V (Fig. 5, Supplementary Fig. S5). Interestingly, the substituted amino acid residues were all hydrophobic even at the third site (A263V), which is predicted to locate on CL1. In Brassicaceae DGAT1, this position is predicted to be within the TM domain. It may be possible that this site and adjacent amino acid residues are peripheral on or partially within the membrane. According to the study of human DGAT1 structure (Wang *et al.*, 2020), a short part of CL1 (IL1 in their report) was predicted to be in

a membrane to form the MBOAT fold (for more detail, see '*Bioinformatics of DGAT1 protein*' below).

Chen *et al*. (2017) reported that the replacement of I447 of BnaDGAT1 with A, C, F, L, T, or V resulted in substantially higher neutral lipid content, whereas the replacement of I447 with D, E, N, R, K or Y resulted in a lower neutral lipid content. Because I, A, C, F, L, and V are hydrophobic amino acid residues, polar amino acids such as D, E, N, R and K are inappropriate to exist within membranes. All DGAT1s tested in this study had 'I' at the corresponding site 447 of BnaDGAT1 (Supplementary Table S5). Chen *et al*. (2017) also mentioned that L441P increased the neutral lipid content. Among the DGAT1s from seven species in this study, GmDGAT1A, AtDGAT1, RcDGAT1 (the 'Low' group), and JcDGAT1 had 'L', whereas VgDGAT1A, HanDGAT1, and SiDGAT1 (the 'High' group) had 'F' at site 441 of BnaDGAT1. L, I, F, and P are all hydrophobic; however, 'F' is an aromatic amino acid, which means it has a bulky benzene ring, but 'L' and 'I' do not (Fig. 4A). This may affect the peptide structure and F146L in GmDGAT1A in this study and I447P in BnaDGAT1 (Chen *et al.*, 2017) increased TAG accumulation likely due to the structural alteration. In their study (2017), the majority of BnaDGAT1 variants with single amino acid residue substitutions that resulted in higher TAG accumulation were either within or close to a TM domain. Exceptions were C286Y on the loop between the TM5 and TM6, G332A on the loop between the TM6 and the TM7, and Y386F on the loop between the TM7 and TM8. Looking at other DGAT1s, corresponding residues of these three amino acids are commonly on the loop region. However, the corresponding amino acid residue of G332A of BnaDGAT1 was originally 'A' in our tested seven DGAT1s. It is unlikely that hydrophobic amino acid residues work efficiently outside the membranes for DGAT1 activity.

In contrast, the double mutations (F149L/F205V, F205V/A263V, F149L/A263V) and the triple mutation (F149L/F205V/A263V) of GmDGAT1A were less effective in increasing TAG content than the single mutations (F149L or A263V) (Fig. 5). However, the GmDGAT1b-MOD reported by Roesler *et al*. (2016) had 13 amino acid substitutions. Chen *et al*. (2017) also reported a single mutation, I447F, which resulted in a higher TAG content than some multiple site mutations of BnaDGAT1 including 2–7 mutations. Given these results and reports, it may be possible that only one amino acid substitution will improve the DGAT ability if it locates at an effective position.

The fatty acid compositions of variants also changed. In particularly, the ratio of palmitoleic acid ($16{:}1^{\Delta 9}$) was significantly decreased and that of other fatty acids increased compared with the native GmDGAT1A (Fig 6A, B). This tendency was observed in DGAT1s of the 'High' group (Fig. 2B). DGAT1s from several species have some differential substrate preferences. However, in general, DGAT1s do not have strong substrate specificities compared with DGAT2s (Demski *et al.*, 2019; Jeppson *et al.*, 2019; Lager *et al.*, 2020; McKeon and He, 2015; Pan, 2013; Shockey *et al.*, 2019; Xu *et al.*, 2014; Xu *et al.*, 2018b; Yu *et al.*, 2008; Yu *et al.*, 2006; Zhou *et al.*, 2013). Higher DGAT expression has been generally found to increase the relative $18{:}1^{\Delta 9}$ and 16:0 contents of the

correspondingly increased TAG apparently reducing further modification of 18:1$^{\Delta 9}$ and 16:0 in the acyl-CoA and DAG pools (Chen *et al.*, 2017; Hatanaka *et al.*, 2016; Roesler *et al.*, 2016).

Bioinformatics of DGAT1 proteins

I-TASSER (Yang and Zhang, 2015; Zhang *et al.*, 2017) is a protein structure prediction and structure-based function annotation web-based server that was ranked on December 2020 as the No. 1 protein structure prediction server in the 14th CASP experiment (https://www.predictioncenter.org/casp14/zscores_final.cgi?gr_type=server_only). I-TASSER simulations generate decoys, which are a large ensemble of structural conformations. Then, I-TASSER uses the SPICKER program to cluster all the decoys based on the pair-wise structure similarity, and reports up to five models that corresponds to the five largest structure clusters. The confidence of each model is quantitatively measured by a C-score (range of [-5, 2]) that is calculated based on the significance of threading template alignments and the convergence parameters of the structure assembly simulations. I-TASSER matches the best confidence model with all structures in the Protein Data Bank (PDB) library by the TM-align structural alignment program and scores them with TM-score. The best match model for VgDGAT1A, GmDGAT1A, and GmDGAT1A-F149L was human DGAT1 (Wang *et al.*, 2020). The TM-scores for VgDGAT1A, GmDGAT1A, and GmDGAT1A-F149L were 0.762, 0.799, and 0.801, respectively. Given these high scores, VgDGAT1A, GmDGAT1A, and GmDGAT1A-F149L proteins in this study have a very similar structure to the human DGAT1 protein. Additionally, the web-based tool can predicted the function of the I-TASSER structure of the target protein through the COACH and COFACTOR programs. The COFACTOR deduces protein functions (Ligand-binding sites, Enzyme Commission numbers and active sites, and Gene Ontology terms) using structure comparison and protein-protein networks and COACH is a meta-server approach that combines multiple function annotation results (on ligand-binding sites) from the COFACTOR, TM-SITE, and S-SITE programs. According to the prediction, the best ligand binding sites for VgDGAT1A was Mn^{2+} (with 1twaA PBD hit and confidence score: 0.09) at ligand binding site residues 277 and 281s (Fig. 7). The best ligand-binding sites for GmDGAT1A were nucleic acids (with 4 × 6aA PBD hit and confidence score: 0.08) at the 372, 375, 377, 380, and 382 ligand binding site residues (Fig. 8A). Also, the best ligand-binding sites for GmDGAT1A-F149L was HEGA-10 (with 2y04B PBD hit and confidence score: 0.06) at the 220 and 221 ligand-binding site residues (Fig. 8B). HEGA-10 is a detergent used for solubilizing protein that has biomolecular interactions with voltage-gated sodium channels (McCusker *et al.*, 2012). Interestingly, the predicted models for all were the same but the ligand-binding sites were absolutely different (Figs. 7 and 8). This difference occurred by single site-directed mutagenesis of F149L for GmDGAT1A. These results are supported by the results of our yeast experiment. Thus, substituting this amino acid has a great role in changing protein function and might lead to the production of more TAG.

DGAT1 belongs to the MBOAT superfamily, which is found in all kingdoms of life. DGAT1 from plants and mammals was previously shown to form a dimer (Caldo *et al.*, 2017; McFie *et al.*, 2010). This dimerization was confirmed by the recent cryo-electron microscopy (cryo-EM) studies of human DAGT1 (Sui *et al.*, 2020; Wang *et al.*, 2020). Each protomer of human DGAT1 has nine trans-membrane (TM) helices, TM1–TM9, with N- and C-termini located on the cytosolic and luminal sides of the ER membrane, respectively. Short helices in the cytosolic loop (CL) and luminal loop (LL) regions orient in parallel to the membrane surface (Wang, *et al*. 2020). This structure is very similar to the topology models of VgDGAT1A and GmDGAT1A (Fig. 4). Crossover of helix TM1 allows the N-terminal CL1 of one protomer to interact with both CL1 and CL2 of the another protomer (Sui *et al.*, 2020). TM2–TM9 and the two CLs, CL2 and CL3 form a distinctive structural fold that called the MBOAT fold (Wang *et al.*, 2020) (Fig. 9). The MBOAT fold of DGAT1 carves out a large hollow chamber within the membrane that is open to the bilayer via a wide lateral gate, and this region is considered as the DGAT1 active site (Sui *et al.*, 2020; Wang *et al.*, 2020). The three amino acid residues in this study face to this reaction chamber (Fig. 9). Of all DGAT1s, the three-dimensional structure of Human DGAT1 is the most investigated using cryo-EM (Sui *et al.*, 2020; Wang *et al.*, 2020). However, their acyl-CoA binding site, DAG binding site, and catalytically active sites are still speculative. Our results reported here can be more completely interpreted when additional discoveries are reported.

In conclusion, our results showed that three amino acids, L174, V230, and V288 in VgDGAT1A; 154L, 210V, and 268V in HanDGAT1; 194L, 250V, and 308V in SiDGAT1; and 154L, 226V and 284V in JcDGAT1, could be key factors of the DGAT1 ‘High’ group’s TAG accumulation (Supplementary Table S4). Also, given the examples of BnaDGAT1 variants (Chen *et al.*, 2017), our results show that a single base change resulting on one single amino acid substitution can be effective in increasing the activities of low performance DGAT1s. As we showed in the primer sequences for site-directed mutagenesis (Supplementary Table S2-2), a single base substitution can increase the TAG accumulation of DGAT1s. This technique can easily be applied to a genome-editing method.

Supplementary data

The following supplementary data are available at *JXB* online.

Table S1. GenBank numbers of genes mentioned in this study.

Table S2. Primer sequences used in the current study.

Table S3. Quantitative gene expression analysis in transgenic Arabidopsis siliques.

Table S4. Corresponding amino acid residue sites, which are numbered on Fig. 3 for various plant DGAT1.

Table S5. Corresponding amino acid residue sites that were tested in BnaDGAT1 (data from Chen *et al.* 2017).

Fig. S1. T2 seed oil contents of individual transgenic lines and the wild-type (WT).

Fig. S2. An example of TLC development of total lipid extracts from transgenic yeast lines (H1246).

Fig. S3. Reverse transcription-PCR of transgenic yeast lines (H1246).

Fig. S4. An example of TLC development of total lipid extracts from transgenic yeast lines (H1246) expressing *GmDGAT1A* variants.

Fig. S5. Quantitative DGAT1 gene expression analysis in transgenic yeast strain H1246.

Fig. S6. A deduced topology model of DGAT1.

Appendix S1. Codon usage biases of DGATs among plants, yeast, and algae.

Acknowledgements

The authors are grateful to Prof. Sten Stymne (Department of Plant Breeding, Swedish University of Agricultural Sciences, Alnarp, Sweden) for providing *S. cerevisiae* H1246 strain. We also thank the students in Laboratory of Crop Science of Kobe University for their great efforts.

Author contributions

TH designed and performed most of the experiments, analyzed the data, and prepared the initial draft of the manuscript; YT performed Arabidopsis transformation and obtained all transgenic lines in this study; DM supervised yeast experiments; HF helped vector constructions and other molecular techniques; DS and TA contributed to valuable discussions during this study; MS worked on bioinformatics; DH supervised this whole study and English editing of the manuscript. All authors contributed to the preparation of the final article.

Conflicts of interest

The authors declare that they have no conflicts of interest with the content of this article.

Data availability

All relevant data can be found within the manuscript and its supplementary data.

References

518 **Anderson MA, Collier L, Dilliplane R, Ayorinde FO**. 1993. Mass Spectrometric characterization of *Vernonia*
519 *galamensis* oil. Journal of the American Oil Chemists' Society **70**, 905-908.
520 **Andrianov V, Borisjuk N, Pogrebnyak N, Brinker A, Dixon J, Spitsin S, Flynn J, Matyszczuk P,**
521 **Andryszak K, Laurelli M, Golovkin M, Koprowski H**. 2010. Tobacco as a production platform for biofuel:
522 overexpression of *Arabidopsis DGAT* and *LEC2* genes increases accumulation and shifts the composition of
523 lipids in green biomass. Plant Biotechnology Journal **8**, 277-287.
524 **Ayorinde FO, Osman G, Shepard RL, Powers FT**. 1988. Synthesis of azelaic acid and suberic acid from
525 *Vernonia galamensis* oil. Jounal of the American Oil Chemits' Society **65**, 1774-1777.
526 **Banilas G, Karampelias M, Makariti I, Kourti A, Hatzopoulos P**. 2011. The olive *DGAT2* gene is
527 developmentally regulated and shares overlapping but distinct expression patterns with *DGAT1*. Journal of
528 Experimental Botany **62**, 521-532.
529 **Bates PD**. 2016. Understanding the control of acyl flux through the lipid metabolic network of plant oil
530 biosynthesis. Biochimica et Biophysica Acta **1861**, 1214-1225.
531 **Beisson F, Koo AJ, Ruuska S, Schwender J, Pollard M, Thelen JJ, Paddock T, Salas JJ, Savage L,**
532 **Milcamps A, Mhaske VB, Cho Y, Ohlrogge JB**. 2003. Arabidopsis genes involved in acyl lipid metabolism.
533 A 2003 census of the candidates, a study of the distribution of expressed sequence tags in organs, and a
534 web-based database. Plant Physiology **132**, 681-697.
535 **Bouvier-Nave P, Benveniste P, Oelkers P, Sturley SL, Hubert S**. 2000. Expression in yeast and tobacco of
536 plant cDNAs encoding acyl CoA:diacylglycerol acyltransferase. European Journal of Biochemstry **267**, 85-96.
537 **Burgal J, Shockey J, Lu C, Dyer J, Larson T, Graham I, Browse J**. 2008. Metabolic engineering of hydroxy
538 fatty acid production in plants: RcDGAT2 drives dramatic increases in ricinoleate levels in seed oil. Plant
539 Biotechnology Journal **6**, 819-831.
540 **Bustos MM, Iyer M, Gagliardi SJ**. 1998. Induction of a ß-phaseolin promoter by exogenous abscisic acid in
541 tobacco: developmental regulation and modulation by external sucrose and Ca^{2+} ions. Plant Molecular Biology
542 **37**, 265-274.
543 **Cagliari A, Margis-Pinheiro M, Loss G, Mastroberti AA, de Araujo Mariath JE, Margis R**. 2010.
544 Identification and expression analysis of castor bean (*Ricinus communis*) genes encoding enzymes from the
545 triacylglycerol biosynthesis pathway. Plant Science **179**, 499-509.
546 **Caldo KMP, Acedo JZ, Panigrahi R, Vederas JC, Weselake RJ, Lemieux MJ**. 2017. Diacylglycerol
547 acyltransferase 1 is regulated by Its N-terminal domain in response to allosteric effectors. Plant Physiology
548 **175**, 667-680.
549 **Carlson KD, Chang SP**. 1985. Chemical eposidation of natural unsaturated epoxy seed oil from *Vernonia*
550 *galamensis* and a look at epoxy oil markets. Jounal of the American Oil Chemits' Society **62**, 934-939.
551 **Carlsson AS**. 2009. Plant oils as feedstock alternatives to petroleum - A short survey of potential oil crop
552 platforms. Biochimie **91**, 665-670.

Carlsson AS, Yilmaz JL, Green AG, Stymne S, Hofvander P. 2011. Replacing fossil oil with fresh oil - with what and for what? European Journal of Lipid Science and Technology **113**, 812-831.

Cases S, Smith SJ, Zheng YW, Myers HM, Lear SR, Sande E, Novak S, Collins C, Welch CB, Lusis AJ, Erickson SK, Farese RV. 1998. Identification of a gene encoding an acyl CoA: diacylglycerol acyltransferase, a key enzyme in triacylglycerol synthesis. Proceedings of the National Academy of Sciences, USA **95**, 13018-13023.

Cases S, Stone SJ, Zhou P, Yen E, Tow B, Lardizabal KD, Voelker T, Farese RV, Jr. 2001. Cloning of DGAT2, a second mammalian diacylglycerol acyltransferase, and related family members. Journal of Biological Chemistry **276**, 38870-38876.

Chen B, Wang J, Zhang G, Liu J, Manan S, Hu H, Zhao J. 2016. Two types of soybean diacylglycerol acyltransferases are differentially involved in triacylglycerol biosynthesis and response to environmental stresses and hormones. Scientific Reports **6**, 28541.

Chen G, Xu Y, Siloto RMP, Caldo KMP, Vanhercke T, Tahchy AE, Niesner N, Chen Y, Mietkiewska E, Weselake RJ. 2017. High-performance variants of plant diacylglycerol acyltransferase 1 generated by directed evolution provide insights into structure function. Plant Journal **92**, 167-177.

Clough SJ, Bent AF. 1998. Floral dip: a simplified method for *Agrobacterium*-mediated transformation of *Arabidopsis thaliana*. Plant Journal **16**, 735-743.

Dahlqvist A, Ståhl U, Lenman M, Banas A, Lee M, Sandager L, Ronne H, Stymne S. 2000. Phospholipid:diacylglycerol acyltransferase: An enzyme that catalyzes the acyl-CoA-independent formation of triacylglycerol in yeast and plants. Proceedings of the National Academy of Sciences, USA **97**, 6487-6492.

Demski K, Jeppson S, Lager I, Misztak A, Jasieniecka-Gazarkiewicz K, Waleron M, Stymne S, Banas A. 2019. Isoforms of acyl-CoA:diacylglycerol acyltransferase2 differ substantially in their specificities toward erucic acid. Plant Physiology **181**, 1468-1479.

Fraser T, Waters A, Chatrattanakunchai S, Stobart K. 2000. Does triacylglycerol biosynthesis require diacylglycerol acyltransferase (DAGAT)? Biochemical Society Transactions **28**, 698-700.

Furmanek T, Demski K, Banas W, Haslam R, Napier J, Stymne S, Banas A. 2014. The utilization of the acyl-CoA and the involvement PDAT and DGAT in the biosynthesis of erucic acid-rich triacylglycerols in Crambe seed oil. Lipids **49**, 327-333.

Gamborg OL, Miller RA, Ojima K. 1968. Nutrient requirements of suspension cultures of soybean root cells. Experimental Cell Research **50**, 151-158.

Hatanaka T, Serson W, Li RZ, Armstrong P, Yu KS, Pfeiffer T, Li XL, Hildebrand D. 2016. A *Vernonia* diacylglycerol acyltransferase can increase renewable oil production. Journal of Agricultural and Food Chemistry **64**, 7188-7194.

Hatanaka T, Yu K, Hildebrand DF. 2003. Cloning and expression of a *Vernonia* and *Euphorbia* diacylglycerol acyltransferase cDNAs. In: Murata N, Yamada M, Nishida I, Okuyama H, Sekiya J, W H, eds. *Advanced research on plant lipids*. Dordrecht, The Netherlands: Kluwer Academic Publishers, 155-158.

He XH, Turner C, Chen GQ, Lin JT, McKeon TA. 2004. Cloning and characterization of a cDNA encoding diacylglycerol acyltransferase from castor bean. Lipids **39**, 311-318.

Hernandez ML, Whitehead L, He Z, Gazda V, Gilday A, Kozhevnikova E, Vaistij FE, Larson TR, Graham IA. 2012. A cytosolic acyltransferase contributes to triacylglycerol synthesis in sucrose-rescued Arabidopsis seed oil catabolism mutants. Plant Physiology **160**, 215-225.

Hobbs DH, Lu CF, Hills MJ. 1999. Cloning of a cDNA encoding diacylglycerol acyltransferase from *Arabidopsis thaliana* and its functional expression. FEBS Letters **452**, 145-149.

Jako C, Kumar A, Wei Y, Zou J, Barton DL, Giblin EM, Covello PS, Taylor DC. 2001. Seed-specific over-expression of an Arabidopsis cDNA encoding a diacylglycerol acyltransferase enhances seed oil content and seed weight. Plant Physiology **126**, 861-874.

Jaworski J, Cahoon EB. 2003. Industrial oils from transgenic plants. Current Opinion in Plant Biology **6**, 178-184.

Jeppson S, Demski K, Carlsson AS, Zhu LH, Banas A, Stymne S, Lager I. 2019. *Crambe hispanica* subsp. *abyssinica* diacylglycerol acyltransferase specificities towards diacylglycerols and acyl-CoA reveal combinatorial effects that greatly affect enzymatic activity and specificity. Frontiers in Plant Science **10**, 1442.

Kalscheuer R, Steinbuchel A. 2003. A novel bifunctional wax ester synthase/acyl-CoA:diacylglycerol acyltransferase mediates wax ester and triacylglycerol biosynthesis in *Acinetobacter calcoaceticus* ADP1. Journal of Biological Chemistry **278**, 8075-8082.

Kawagoe Y, Campell BR, Murai N. 1994. Synergism between CACGTG (G-box) and CSCCTG *cis*-elements is required for activation of the bean seed storage protein ß-phaseolin gene. Plant Journal **5**, 885-890.

King A, Nam JW, Han J, Hilliard J, Jaworski JG. 2007. Cuticular wax biosynthesis in petunia petals: cloning and characterization of an alcohol-acyltransferase that synthesizes wax-esters. Planta **226**, 381-394.

Kroon JT, Wei W, Simon WJ, Slabas AR. 2006. Identification and functional expression of a type 2 acyl-CoA:diacylglycerol acyltransferase (DGAT2) in developing castor bean seeds which has high homology to the major triglyceride biosynthetic enzyme of fungi and animals. Phytochemistry **67**, 2541-2549.

Lager I, Jeppson S, Gippert AL, Feussner I, Stymne S, Marmon S. 2020. Acyltransferases regulate oil quality in *Camelina sativa* through both acyl donor and acyl acceptor specificities. Frontiers in Plant Science **11**, 1144.

Lardizabal K, Effertz R, Levering C, Mai J, Pedroso MC, Jury T, Aasen E, Gruys K, Bennett K. 2008. Expression of *Umbelopsis ramanniana DGAT2A* in seed increases oil in soybean. Plant Physiology **148**, 89-96.

Lardizabal KD, Mai JT, Wagner NW, Wyrick A, Voelker T, Hawkins DJ. 2001. DGAT2 is a new diacylglycerol acyltransferase gene family: purification, cloning, and expression in insect cells of two polypeptides from *Mortierella ramanniana* with diacylglycerol acyltransferase activity. Journal of Biological Chemistry **276**, 38862-38869.

Li F, Wu X, Lam P, Bird D, Zheng H, Samuels L, Jetter R, Kunst L. 2008. Identification of the wax ester synthase/acyl-coenzyme A: diacylglycerol acyltransferase WSD1 required for stem wax ester biosynthesis in Arabidopsis. Plant Physiology **148**, 97-107.

Li M, Zhao M, Wu H, Wu W, Xu Y. 2013a. Cloning, characterization and functional analysis of two type 1 diacylglycerol acyltransferases (DGAT1s) from Tetraena mongolica. Journal of Integrative Plant Biology **55**, 490-503.

Li R, Hatanaka T, Yu K, Wu Y, Fukushige H, Hildebrand D. 2013b. Soybean oil biosynthesis: role of diacylglycerol acyltransferases. Functional and Integrative Genomics **13**, 99-113.

Li R, Yu K, Hatanaka T, Hildebrand DF. 2010a. *Vernonia* DGATs increase accumulation of epoxy fatty acids in oil. Plant Biotechnology Journal **8**, 184-195.

Li R, Yu K, Hildebrand DF. 2010b. *DGAT1*, *DGAT2* and *PDAT* expression in seeds and other tissues of epoxy and hydroxy fatty acid accumulating plants. Lipids **45**, 145-157.

Li R, Yu K, Wu Y, Tateno M, Hatanaka T, Hildebrand DF. 2012. *Vernonia* DGATs can complement the disrupted oil and protein metabolism in epoxygenase-expressing soybean seeds. Metabolic Engineering **14**, 29-38.

Lung S-C, Weselake RJ. 2006. Diacylglycerol acyltransferase: A key mediator of plant triacylglycerol Ssynthesis. Lipids **41**, 1073-1088.

McCusker EC, Bagneris C, Naylor CE, Cole AR, D'Avanzo N, Nichols CG, Wallace BA. 2012. Structure of a bacterial voltage-gated sodium channel pore reveals mechanisms of opening and closing. Nature Communications **3**, 1102.

McFie PJ, Stone SL, Banman SL, Stone SJ. 2010. Topological orientation of acyl-CoA:diacylglycerol acyltransferase-1 (DGAT1) and identification of a putative active site histidine and the role of the n terminus in dimer/tetramer formation. Journal of Biological Chemistry **285**, 37377-37387.

McGinn M, Phippen WB, Chopra R, Bansal S, Jarvis BA, Phippen ME, Dorn KM, Esfahanian M, Nazarenus TJ, Cahoon EB, Durrett TP, Marks MD, Sedbrook JC. 2019. Molecular tools enabling pennycress (*Thlaspi arvense*) as a model plant and oilseed cash cover crop. Plant Biotechnology Journal **17**, 776-788.

McKeon TA, He XH. 2015. Castor diacylglycerol acyltransferase type 1 (DGAT1) displays greater activity with diricinolein than Arabidopsis DGAT1. Biocatalysis and Agricultural Biotechnology **4**, 276-278.

Misra A, Khan K, Niranjan A, Nath P, Sane VA. 2013. Over-expression of *JcDGAT1* from *Jatropha curcas* increases seed oil levels and alters oil quality in transgenic *Arabidopsis thaliana*. Phytochemistry **96**, 37-45.

Murashige T, Skoog F. 1962. A revised medium for rapid growth and bio assays with tobacco tissue cultures. Physiologia Plantarum **15**, 473-497.

Neff WE, Adlof RO, Konishi H, Weisleder D. 1993. High-performance liquid chromatography of the triacylglycerols of *Vernonia galamensis* and *Crepis alpina* seed oils. Journal of the American Oil Chemists' Society **70**, 449-455.

Nykiforuk CL, Tara L. Furukawa-Sto¡er, Phillip W. Hu¡, Magdalena Sarna, Andre¨ Laroche, Maurice M. Moloney, Weselake RJ. 2002. Characterization of cDNAs encoding diacylglycerol acyltransferase from cultures of *Brassica napus* and sucrose-mediated induction of enzyme biosynthesis. Biochimica et Biophysica Acta **1580**, 95-109.

664 **Oelkers P, Tinkelenberg A, Erdeniz N, Cromleyi D, Billheimeri JT, Sturley SL**. 2000. A lecithin cholesterol
665 acyltransferase-like gene mediates diacylglycerol esterification in yeast. Journal of Biological Chemistry **275**,
666 15609-15612.
667 **Ohlrogge J, Browse J**. 1995. Lipid biosynthesis. Plant Cell **7**, 957-970.
668 **Ohlrogge JB**. 1994. Design of new plant products: Engineering of fatty acid metabolism. Plant Physiology
669 **104**, 821-826.
670 **Omasits U, Ahrens CH, Muller S, Wollscheid B**. 2014. Protter: interactive protein feature visualization and
671 integration with experimental proteomic data. Bioinformatics **30**, 884-886.
672 **Pan X**. 2013. Indentification of a pair of phospholipid:diacylglycerol acyltransferases from developing flax
673 (*Linum trilinolenin* L.) seed catalyzing the selective production of trilinolenin. Journal of Biological Chemistry
674 **288**, 24173-24188.
675 **Perdue REJ, Carlson KD, Gilbert MG**. 1986. *Vernonia galamensis*, potential new crop source of epoxy acid.
676 Economic Botany **40**, 54-68.
677 **Rao SS, Hildebrand D**. 2009. Changes in oil content of transgenic soybeans expressing the yeast *SLC1*
678 gene. Lipids **44**, 945-951.
679 **Regmi A, Shockey J, Kotapati HK, Bates PD**. 2020. Oil-producing metabolons containing DGAT1 use
680 separate substrate pools from those containing DGAT2 or PDAT. Plant Physiology **184**, 720-737.
681 **Roesler K, Shen B, Bermudez E, Li C, Hunt J, Damude HG, Ripp KG, Everard JD, Booth JR, Castaneda**
682 **L, Feng L, Meyer K**. 2016. An improved variant of soybean type 1 diacylglycerol acyltransferase increases
683 the oil content and decreases the soluble carbohydrate content of soybeans. Plant Physiology **171**, 878-893.
684 **Rosli R, Chan PL, Chan KL, Amiruddin N, Low EL, Singh R, Harwood JL, Murphy DJ**. 2018. In silico
685 characterization and expression profiling of the diacylglycerol acyltransferase gene family (DGAT1, DGAT2,
686 DGAT3 and WS/DGAT) from oil palm, *Elaeis guineensis*. Plant Science **275**, 84-96.
687 **Saha S, Enugutti B, Rajakumari S, Rajasekharan R**. 2006. Cytosolic triacylglycerol biosynthetic pathway in
688 oilseeds. Molecular cloning and expression of peanut cytosolic diacylglycerol acyltransferase. Plant
689 Physiology **141**, 1533-1543.
690 **Sandager L, Gustavsson MH, Stahl U, Dahlqvist A, Wiberg E, Banas A, Lenman M, Ronne H, Stymne S**.
691 2002. Storage lipid synthesis is non-essential in yeast. Journal of Biological Chemistry **277**, 6478-6482.
692 **Sanjaya, Miller R, Durrett TP, Kosma DK, Lydic TA, Muthan B, Koo AJ, Bukhman YV, Reid GE, Howe**
693 **GA, Ohlrogge J, Benning C**. 2013. Altered lipid composition and enhanced nutritional value of *Arabidopsis*
694 leaves following introduction of an algal diacylglycerol acyltransferase 2. Plant Cell **25**, 677-693.
695 **Shockey J, Lager I, Stymne S, Kotapati HK, Sheffield J, Mason C, Bates PD**. 2019. Specialized
696 lysophosphatidic acid acyltransferases contribute to unusual fatty acid accumulation in exotic *Euphorbiaceae*
697 seed oils. Planta **249**, 1285-1299.
698 **Shockey JM, Gidda SK, Chapital DC, Kuan JC, Dhanoa PK, Bland JM, Rothstein SJ, Mullen RT, Dyer**
699 **JM**. 2006. Tung tree DGAT1 and DGAT2 have nonredundant functions in triacylglycerol biosynthesis and are
700 localized to different subdomains of the endoplasmic reticulum. Plant Cell **18**, 2294-2313.

Siloto RM, Truksa M, Brownfield D, Good AG, Weselake RJ. 2009. Directed evolution of acyl-CoA:diacylglycerol acyltransferase: development and characterization of *Brassica napus DGAT1* mutagenized libraries. Plant Physiology and Biochemistry **47**, 456-461.

Stahl U, Carlsson AS, Lenman M, Dahlqvist A, Huang B, Banas W, Banas A, Stymne S. 2004. Cloning and functional characterization of a phospholipid:diacylglycerol acyltransferase from Arabidopsis. Plant Physiology **135**, 1324-1335.

Stobart K, Manuel Mancha, Marit Lenman, Anders Dahlqvist, Stymne S. 1997. Triacylglycerols are synthesised and utilized by transacylation reactions in microsomal preparations of developing safflower (*Carthamus tinctorius L.) seeds*. Planta **203**, 58-66.

Sui X, Wang K, Gluchowski NL, Elliott SD, Liao M, Walther TC, Farese RV, Jr. 2020. Structure and catalytic mechanism of a human triacylglycerol-synthesis enzyme. Nature **581**, 323-328.

Taylor DC, Zhang Y, Kumar A, Francis T, Giblin EM, Barton DL, Ferrie JR, Laroche A, Shah S, Zhu W, Snyder CL, Hall L, Rakow G, Harwood JL, Weselake RJ. 2009. Molecular modification of triacylglycerol accumulation by over-expression of *DGAT1* to produce canola with increased seed oil content under field conditions. Botany **87**, 533-543.

Troncoso-Ponce MA, Kilaru A, Cao X, Durrett TP, Fan J, Jensen JK, Thrower NA, Pauly M, Wilkerson C, Ohlrogge JB. 2011. Comparative deep transcriptional profiling of four developing oilseeds. Plant Journal **68**, 1014-1027.

Tuechetto-Zolet AC, Marashin F, de Morais GL, Cagliari A, Andrade CM, Margis-Pinheiro M, Rogerio M. 2011. Evolutionary view of acyl-CoA diacylglycerol acyltransferase (DGAT), a key enzyme in neutral lipid biosynthesis. BMC Evolutionary Biology **11**.

Wang L, Qian H, Nian Y, Han Y, Ren Z, Zhang H, Hu L, Prasad BVV, Laganowsky A, Yan N, Zhou M. 2020. Structure and mechanism of human diacylglycerol *O*-acyltransferase 1. Nature **581**, 329-332.

Wang Z, Huang W, Chang J, Sebastian A, Li Y, Li H, Wu X, Zhang B, Meng F, Li W. 2014. Overexpression of *SiDGAT1*, a gene encoding acyl-CoA:diacylglycerol acyltransferase from *Sesamum indicum* L. increases oil content in transgenic Arabidopsis and soybean. Plant Cell, Tissue and Organ Culture **119**, 399-410.

Xu J, Francis T, Mietkiewska E, Giblin EM, Barton DL, Zhang Y, Zhang M, Taylor DC. 2008. Cloning and characterization of an acyl-CoA-dependent *diacylglycerol acyltransferase 1* (*DGAT1*) gene from *Tropaeolum majus*, and a study of the functional motifs of the DGAT protein using site-directed mutagenesis to modify enzyme activity and oil content. Plant Biotechnology Journal **6**, 799-818.

Xu JY, Kazachkov M, Jia YH, Zheng ZF, Zou JT. 2013. Expression of a type 2 diacylglycerol acyltransferase from *Thalassiosira pseudonana* in yeast leads to incorporation of docosahexaenoic acid beta-oxidation intermediates into triacylglycerol. FEBS Journal **280**, 6162-6172.

Xu RH, Yang TQ, Wang RL, Liu AZ. 2014. Characterisation of *DGAT1* and *DGAT2* from *Jatropha curcas* and their functions in storage lipid biosynthesis. Functional Plant Biology **41**, 321-329.

Xu Y, Caldo KMP, Pal-Nath D, Ozga J, Lemieux MJ, Weselake RJ, Chen GQ. 2018a. Properties and biotechnological applications of acyl-CoA:diacylglycerol acyltransferase and phospholipid:diacylglycerol acyltransferase from terrestrial plants and microalgae. Lipids **53**, 663-688.

Xu Y, Holic R, Li DR, Pan X, Mietkiewska E, Chen GQ, Ozga J, Weselake RJ. 2018b. Substrate preferences of long-chain acyl-CoA synthetase and diacylglycerol acyltransferase contribute to enrichment of flax seed oil with α-linolenic acid. Biochemical Journal **475**, 1473-1489.

Xu Y, Pan X, Lu J, Wang J, Shan Q, Stout J, Chen G. 2021. Evolutionary and biochemical characterization of a *Chromochloris zofingiensis* MBOAT with wax synthase and diacylglycerol acyltransferase activity. Journal of Experimental Botany **72**, 5584-5598.

Yang J, Zhang Y. 2015. I-TASSER server: new development for protein structure and function predictions. Nucleic Acids Research **43**, W174-181.

Yu K, Li R, Hatanaka T, Hildebrand D. 2008. Cloning and functional analysis of two type 1 diacylglycerol acyltransferases from *Vernonia galamensis*. Phytochemistry **69**, 1119-1127.

Yu KS, McCracken CT, Li RZ, Hildebrand DF. 2006. Diacylglycerol acyltransferases from *Vernonia* and *Stokesia* prefer substrates with vernolic acid. Lipids **41**, 557-566.

Zhang C, Freddolino PL, Zhang Y. 2017. COFACTOR: improved protein function prediction by combining structure, sequence and protein-protein interaction information. Nucleic Acids Research **45**, W291-W299.

Zhao YP, Wu N, Li WJ, Shen JL, Chen C, Li FG, Hou YX. 2021. Evolution and characterization of acetyl Coenzyme A: diacylglycerol acyltransferase genes in cotton identify the roles of *GhDGAT3D* in oil biosynthesis and fatty acid composition. Genes (Basel) **12**.

Zhou XR, Shrestha P, Yin F, Petrie JR, Singh SP. 2013. AtDGAT2 is a functional acyl-CoA:diacylglycerol acyltransferase and displays different acyl-CoA substrate preferences than AtDGAT1. FEBS Letters **587**, 2371-2376.

Zou J, Wei Y, Jaco C, Kumar A, Selvaraj G, Taylor DC. 1999. The *Arabidopsis thaliana TAG1* mutant has a mutation in a diacylglycerol acyltransferase gene. Plant Journal **19**, 645-653.

762 **Figure legends**

763

764 **Fig. 1**. Wild-type (WT) and T3 seed oil contents (A) and the major fatty acid compositions (B) of
765 exogenous *DGAT1* gene expressing Arabidopsis lines.
766 Two individual lines of each *DGAT1*-introduced plants were grown and the mature T3 seeds
767 were harvested. WT, wild-type; AtD-OE-4 and AtD-0E-6, *AtDGAT1* over-expression lines;
768 RcD-4 and RcD-10, *RcDGAT1* expressing lines; GmD-1 and GmD-3, *GmDGAT1A* expressing
769 lines; VgD-10 and VgD-12, *VgDGAT1A* expressing lines, respectively. Values indicate the mean
770 ± SD (n = 3 ~ 5). (A) Wild-type (WT) and T3 seed oil contents. *Different letters* indicate a
771 significant difference (p<0.05) between transgenic lines based on Tukey's HSD test. (B) Major
772 fatty acid compositions of T3 seed oil contents of WT and exogenous *DGAT1*-expressing
773 Arabidopsis lines. 16:0, palmitic acid; 18:0, stearic acid; 18:1, oleic acid; 18:2, linoleic acid; 18:3,
774 α-linolenic acid; 20:1, eicosenoic acid. Others include palmitoleic acid ($16:1^{\Delta 9}$), arachidic acid
775 (20:0), eicosadienoic acid ($20:2^{\Delta 11,14}$), Eicosatrienoic acid ($20:3^{\Delta 11,14,17}$), behenic acid (22:0), erucic
776 acid ($22:1^{\Delta 13}$), lignoceric acid (24:0), and nervonic acid ($24:1^{\Delta 15}$) those contents were less than
777 1.8%.

778

779 **Fig. 2**. Oil content and fatty acid composition of yeast (H1246) transgenic lines measured by GC.
780 (A) Total lipid (blue column) and TAG (red column) contents. (B) Fatty acid compositions in
781 total lipid. 16:0, palmitic acid; 16:1, palmitoleic acid; 18:0, stearic acid; 18:1, oleic acid.
782 VC, empty vector control; At, *AtDGAT1*; Rc, *RcDGAT1*; Gm, *GmDGAT1A*; Vg, *VgDGAT1A*;
783 Ha, *HanDGAT1*; Jc, *JcDGAT1*; *Si, SiDGAT1* expressing lines, respectively. Values represent the
784 means ± S.E. of 5~13 replications. There were significant differences between the "Low" group
785 and the "High" group in both total lipid and in TAG based on Tukey's HSD test (p<0.05) .

786

787 **Fig. 3**. Amino acid sequence alignment of VgDGAT1A, HanDGAT1, SiDGAT1, JcDGAT1,
788 RcDGAT1, AtDGAT1, GmDGAT1A and BnaDGAT1.
789 Red arrows indicate the different amino acid residues between the upper four (the "High" group)
790 and the lower four. Black lines show trans-membrane domains of upper six DGAT1s and blue
791 lines show trans-membrane domains of lower two DGAT1s of Brassicaceae family. Trans-
792 membrane domains were predicted by Phobius.

793

794 **Fig. 4**. The predicted topology models of VgDGAT1A (A) and (B) GmDGAT1A created by
795 Protter (Omasits *et al.*, 2014).
796 The trans-membrane domains were predicted by Phobius. TM, trans-membrane domain; CL,
797 cytosolic loop; LL, ER luminal loop. Residues in color indicate that Red, residues for substitution;
798 Pink, putative active site; Green, dimer forming interface; Blue, putative acyl-CoA binding site;
799 Purple, putative DAG binding site. Yellow circles indicate amino acid residues tested in

BnaDGAT1 (Chen *et al.*, 2017). Putative functional sites are according to several reports (Chen *et al.*, 2017; Sui *et al.*, 2020; Wang *et al.*, 2020). (A) VgDGAT1A. Red numbers and arrows are predicted key amino acid residues in this study. (B) GmDGAT1A. Site-directed amino acid substitutions are shown in red letters.

Fig. 5. Total lipid (blue column) and TAG (red column) contents of yeast H1246 strains hosting *GmDGAT1A* variants generated by site-directed mutagenesis.
VC, empty vector control; Gm, native GmDGAT1A, and GmDGAT1A variants, F149L, F205V, A263V, F149L/F205V, F205V/A263V, F149L/A263V; Triple means F149L/F205V/A263V. Oil contents of the yeast (H1246) cells were analyzed by GC-FID. *Different letters* indicate a significant difference (p<0.05) between variant lines based on Tukey's HSD test (n = 5).

Fig. 6. Fatty acid composition in total lipid (A) and TAG fraction (B) of yeast H1246 strains hosting *GmDGAT1A* variants generated by site-directed mutagenesis.
VC, empty vector control; Gm, native GmDGAT1A; GmDGAT1A variants are same as in Fig. 5. Fatty acids of the yeast cells were analyzed by GC-FID. *Different letters* indicate a significant difference (p<0.05) between variant lines based on Tukey's HSD test (n = 5).

Fig. 7. Two view pictures of ligand binding site residues for VgDGAT1A.
Atomic view (A) and ribbon view (B) with manganese (2+) ligand binding site at 277 and 281 residues (red arrows).

Fig. 8. Two view pictures of ligand binding site residues for GmDGAT1A (A) and GmDGAT1A-F149L (B).
A. Top, Atomic view; bottom, ribbon view of GmDGAT1A with nucleic acid ligand binding site at 372, 375, 377, 380 and 382 residues. B. Top, Atomic view; bottom, ribbon view of GmDGAT1A-F149L with HEGA-10 ligand binding site at 220 and 221 residues (red arrows).

Fig. 9. Three-dimensional structures of VgDGAT1A, GmDGAT1A, and GmDGAT1A-F149L.
Cartoons represent each DGAT1 protomer in two orientations. The MBOAT fold is marked with a red dashed circle.

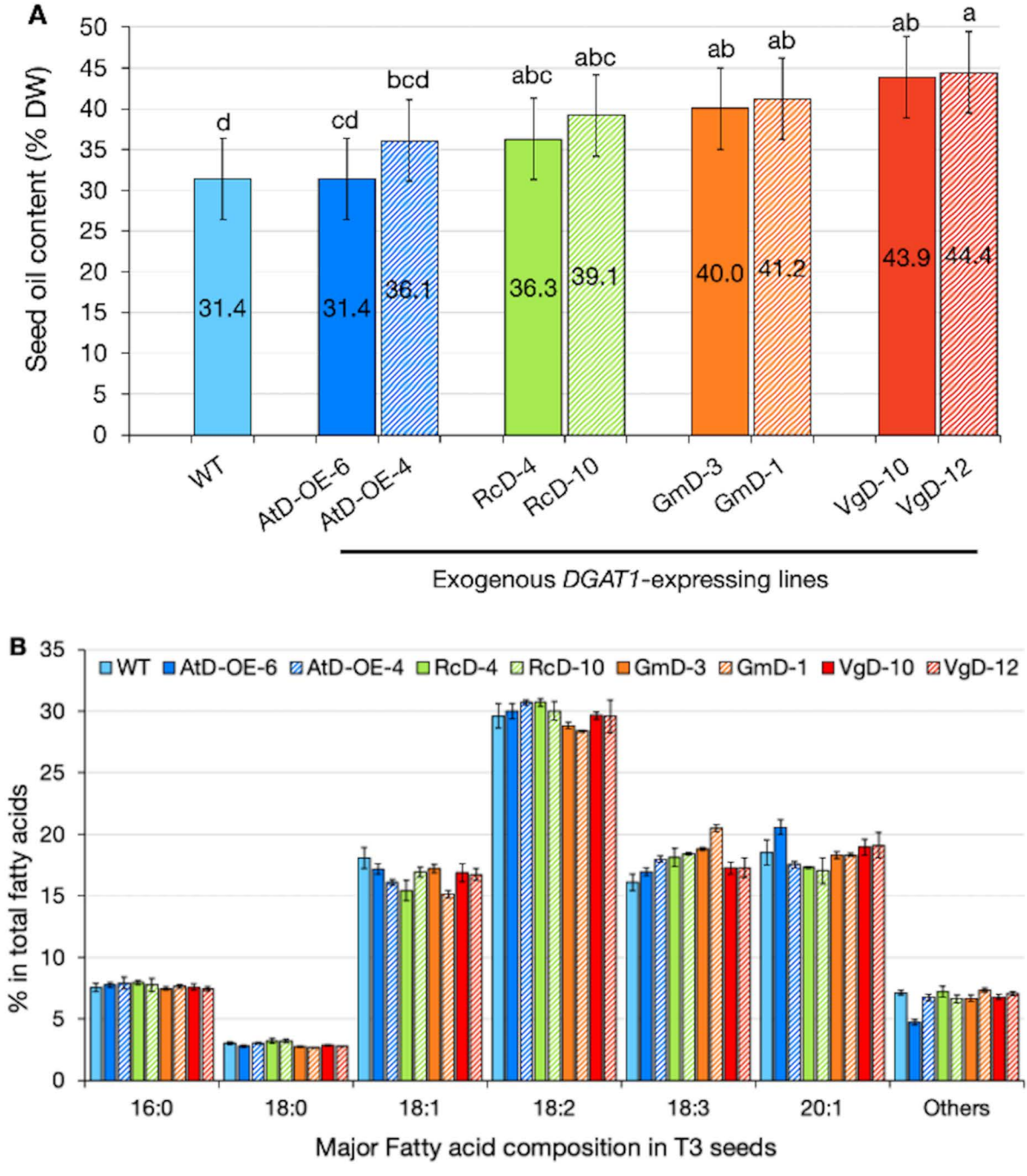
A
Seed oil content (% DW)
50
45
40
35
30
25
20
15
10
5
0
d
cd
bcd
abc
abc
ab
ab
ab
a
31.4
31.4
36.1
36.3
39.1
40.0
41.2
43.9
44.4
WT
AtD-OE-6
AtD-OE-4
RcD-4
RcD-10
GmD-3
GmD-1
VgD-10
VgD-12
Exogenous DGAT1-expressing lines
B
WT
AtD-OE-6
AtD-OE-4
RcD-4
RcD-10
GmD-3
GmD-1
VgD-10
VgD-12
% in total fatty acids
35
30
25
20
15
10
5
0
16:0
18:0
18:1
18:2
18:3
20:1
Others
Major Fatty acid composition in T3 seeds

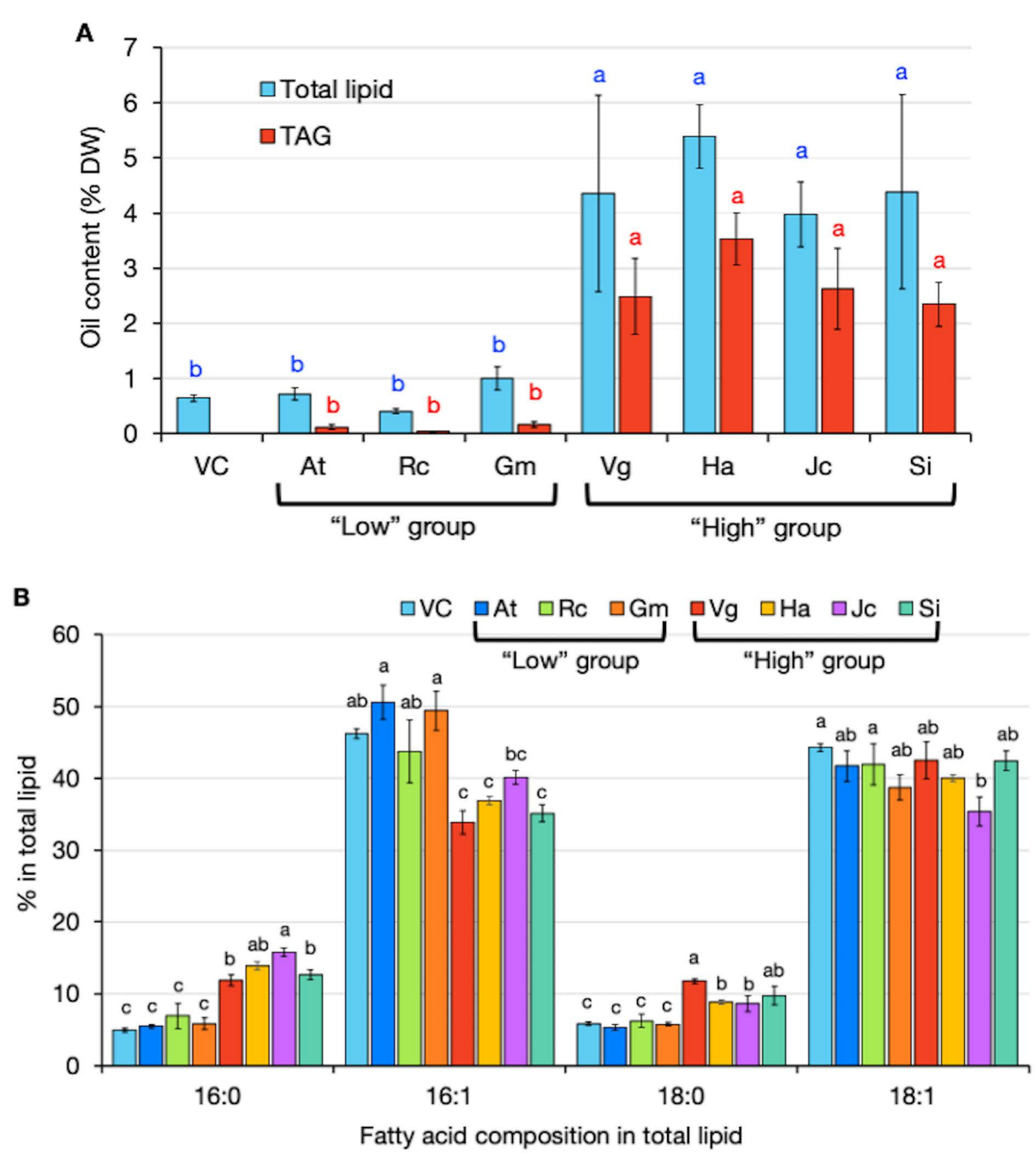
A
Oil content (% DW)
Total lipid
TAG
VC
At
Rc
Gm
Vg
Ha
Jc
Si
"Low" group
"High" group
B
% in total lipid
16:0
16:1
18:0
18:1
Fatty acid composition in total lipid

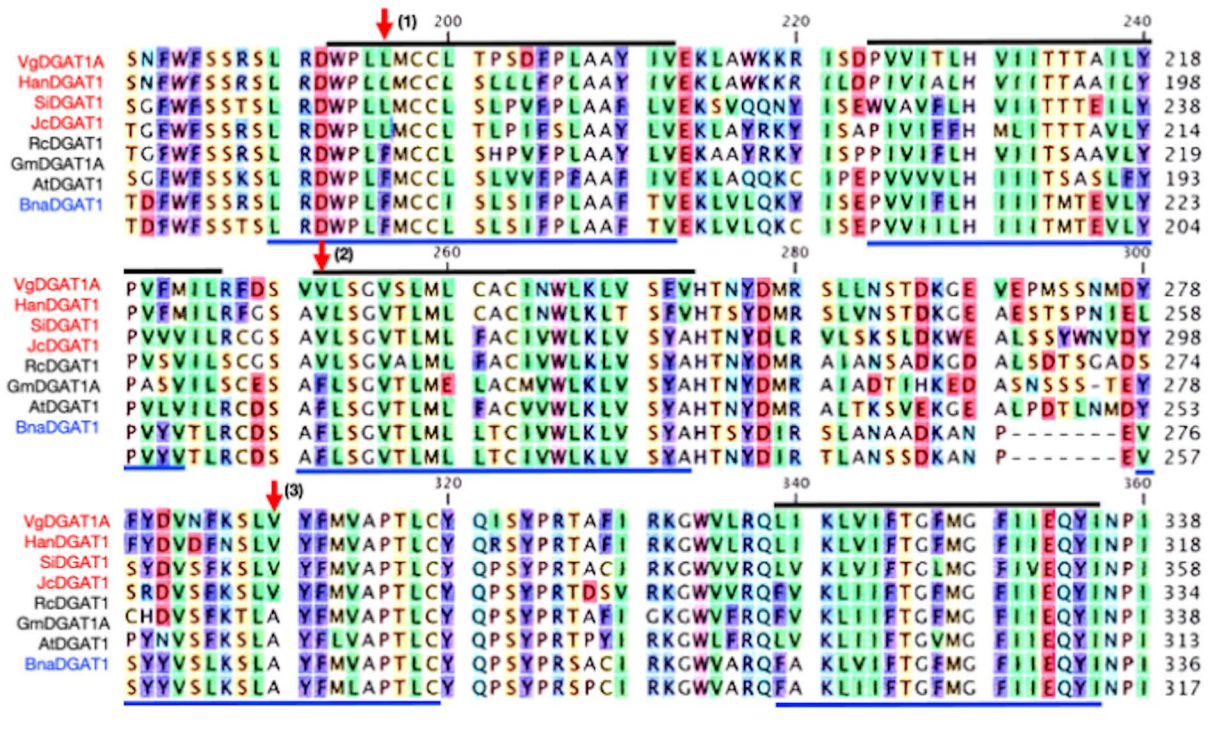
(1)
(2)
(3)
VgDGAT1A
HanDGAT1
SiDGAT1
JcDGAT1
RcDGAT1
GmDGAT1A
AtDGAT1
BnaDGAT1

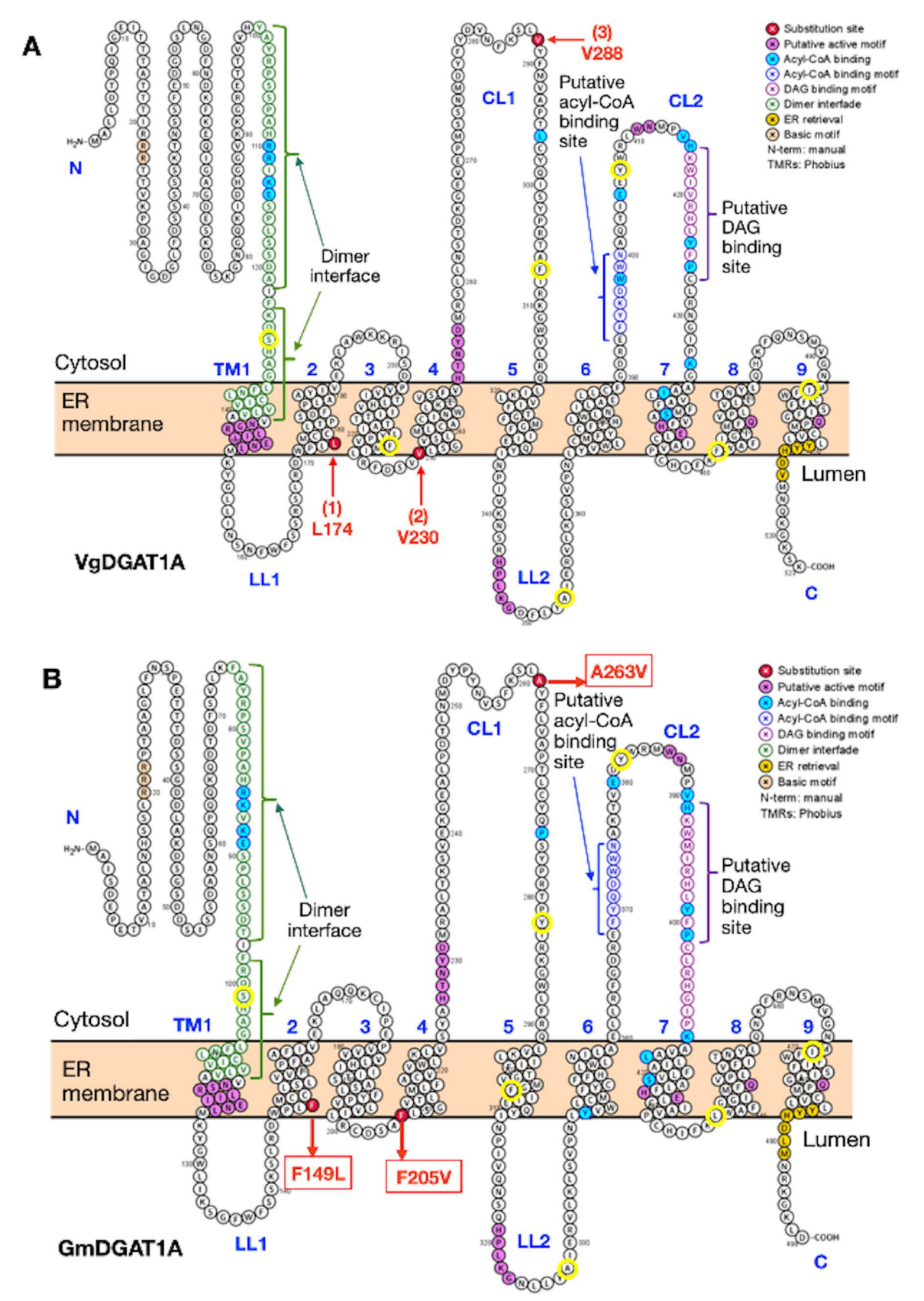
A
Substitution site
Putative active motif
Acyl-CoA binding
Acyl-CoA binding motif
DAG binding motif
Dimer interface
ER retrieval
Basic motif
N-term: manual
TMRs: Phobius
(3)
V288
CL1
Putative
acyl-CoA
binding
site
CL2
N
Putative
DAG
binding
site
Dimer
interface
Cytosol
TM1
2
3
4
5
6
7
8
9
ER
membrane
Lumen
(1)
L174
(2)
V230
VgDGAT1A
LL1
LL2
C
B
A263V
Putative
acyl-CoA
binding
site
CL1
CL2
N
Putative
DAG
binding
site
Dimer
interface
Cytosol
TM1
2
3
4
5
6
7
8
9
ER
membrane
Lumen
F149L
F205V
GmDGAT1A
LL1
LL2
C

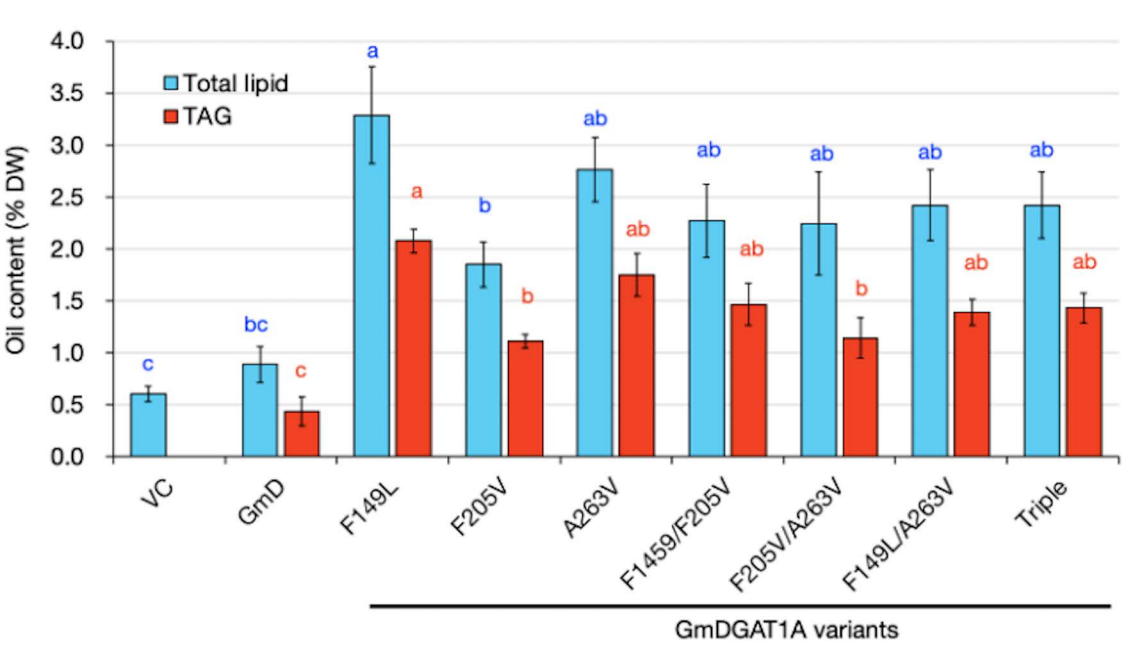
Oil content (% DW)
4.0
3.5
3.0
2.5
2.0
1.5
1.0
0.5
0.0
Total lipid
TAG
a
a
b
b
ab
ab
ab
ab
ab
ab
ab
ab
ab
ab
bc
c
c
c
VC
GmD
F149L
F205V
A263V
F1459/F205V
F205V/A263V
F149L/A263V
Triple
GmDGAT1A variants

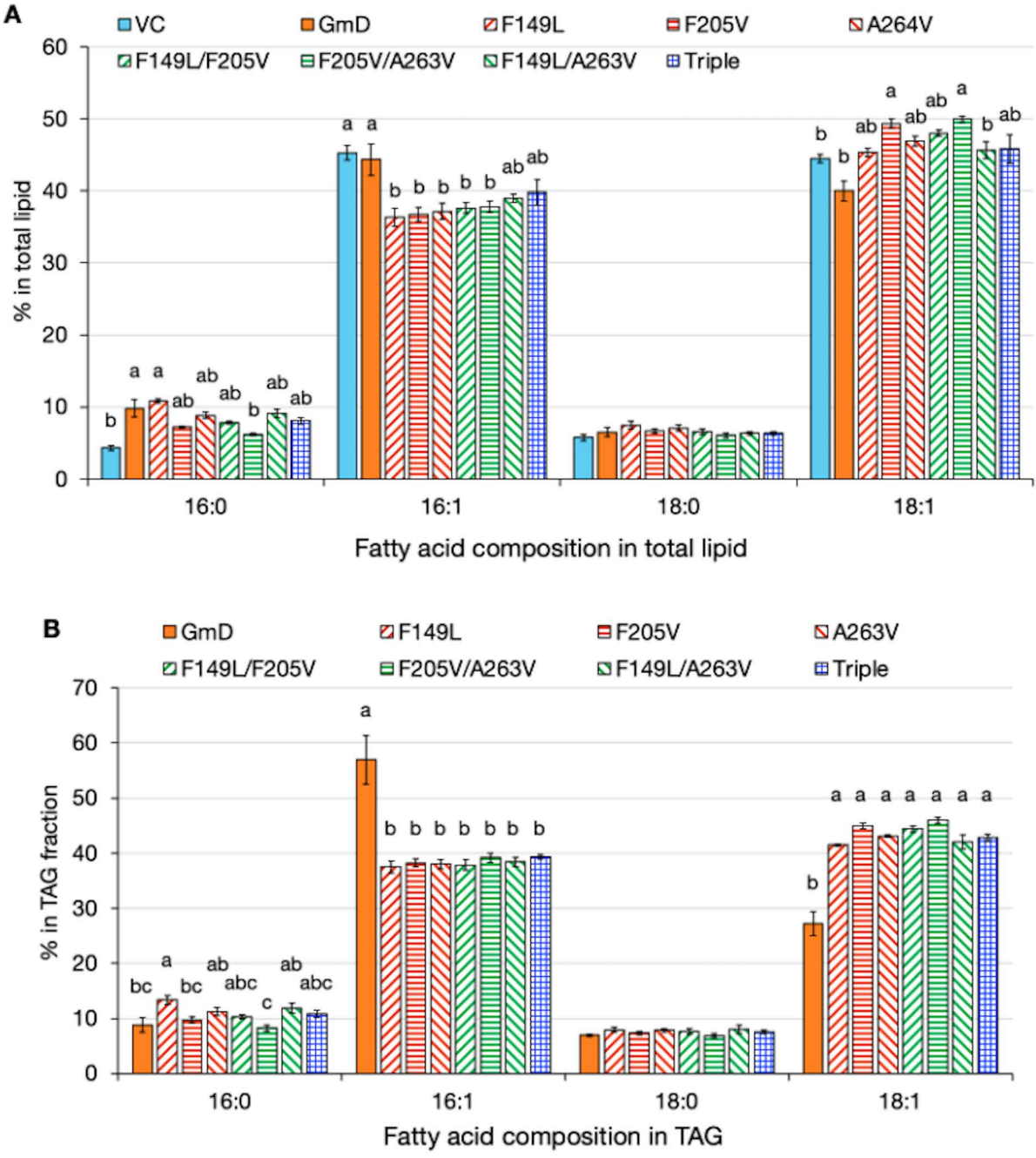
A
VC
GmD
F149L
F205V
A264V
F149L/F205V
F205V/A263V
F149L/A263V
Triple
% in total lipid
Fatty acid composition in total lipid
16:0
16:1
18:0
18:1
B
GmD
F149L
F205V
A263V
F149L/F205V
F205V/A263V
F149L/A263V
Triple
% in TAG fraction
Fatty acid composition in TAG

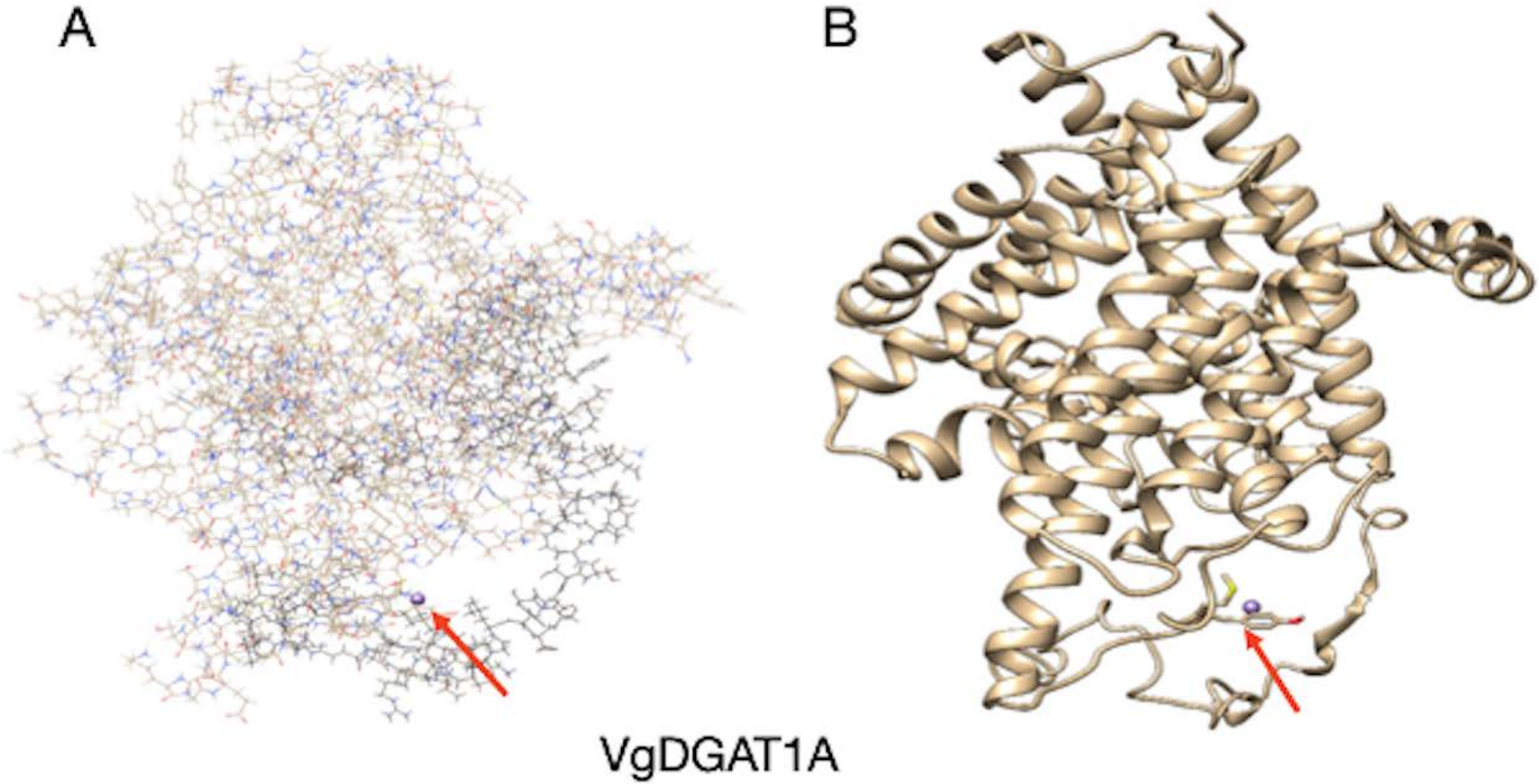
A
B
VgDGAT1A

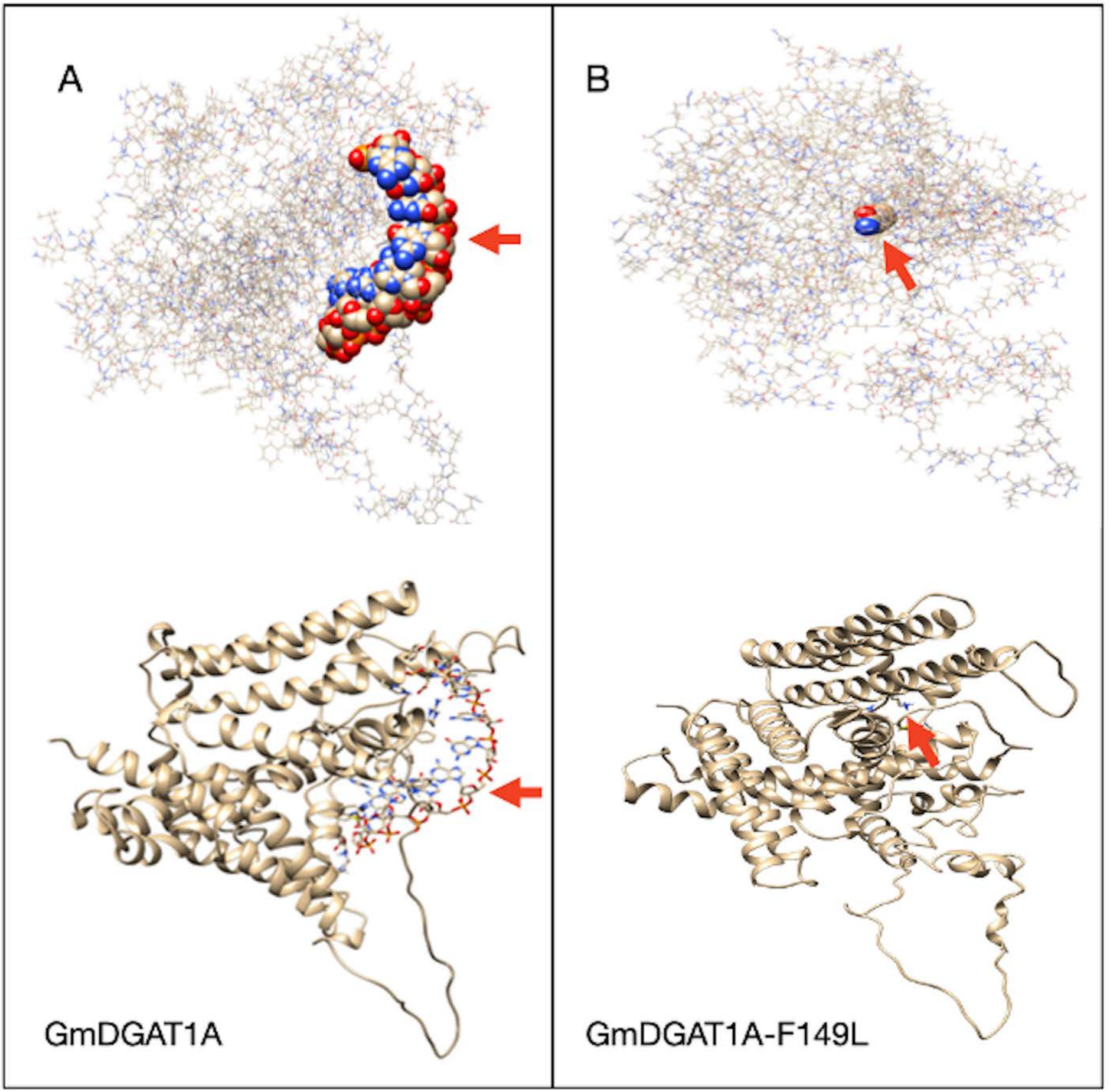
A
B
GmDGAT1A
GmDGAT1A-F149L

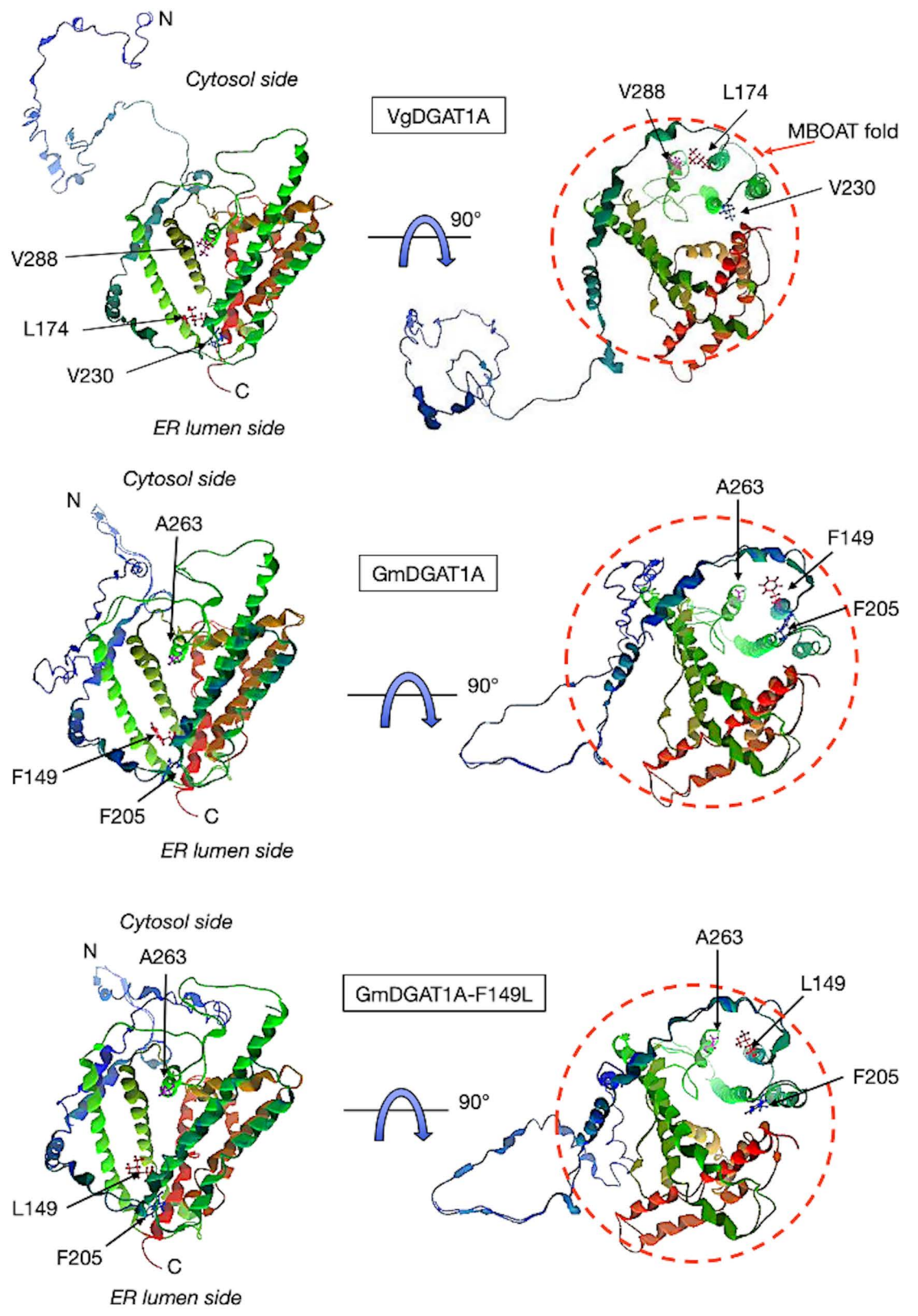
N
Cytosol side
V288
L174
V230
C
ER lumen side
VgDGAT1A
90°
V288
L174
MBOAT fold
V230
Cytosol side
N
A263
F149
F205
C
ER lumen side
GmDGAT1A
90°
A263
F149
F205
Cytosol side
N
A263
L149
F205
C
ER lumen side
GmDGAT1A-F149L
90°
A263
L149
F205